Supporting Information

The Atropisomeric Dynamic Behaviour of Symmetrical *N*-acylated Amine-Bridged Calix[4]arenes

Martin Tlustý,[†] Václav Eigner,[§] Hana Dvořáková[∫] and Pavel Lhoták[†*]

[†]Department of Organic Chemistry, University of Chemistry and Technology, Prague (UCTP), Technická 5, 166 28 Prague 6, Czech Republic
[§]Department of Solid State Chemistry, UCTP, Technická 5, 166 28 Prague 6, Czech Republic
[∫]Laboratory of NMR Spectroscopy, UCTP, Technická 5, 166 28 Prague 6, Czech Republic.

Table of Contents

1. Spectral characterization of compounds

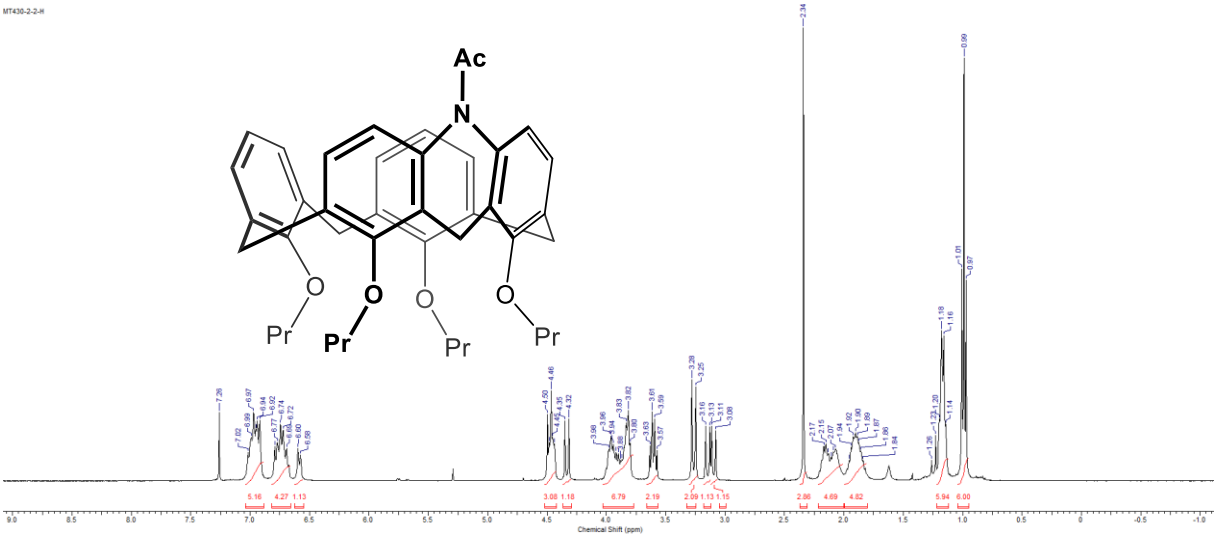

Figure S1: ^{1}H NMR of compound **7a** ($CDCl_3$, 400 MHz).

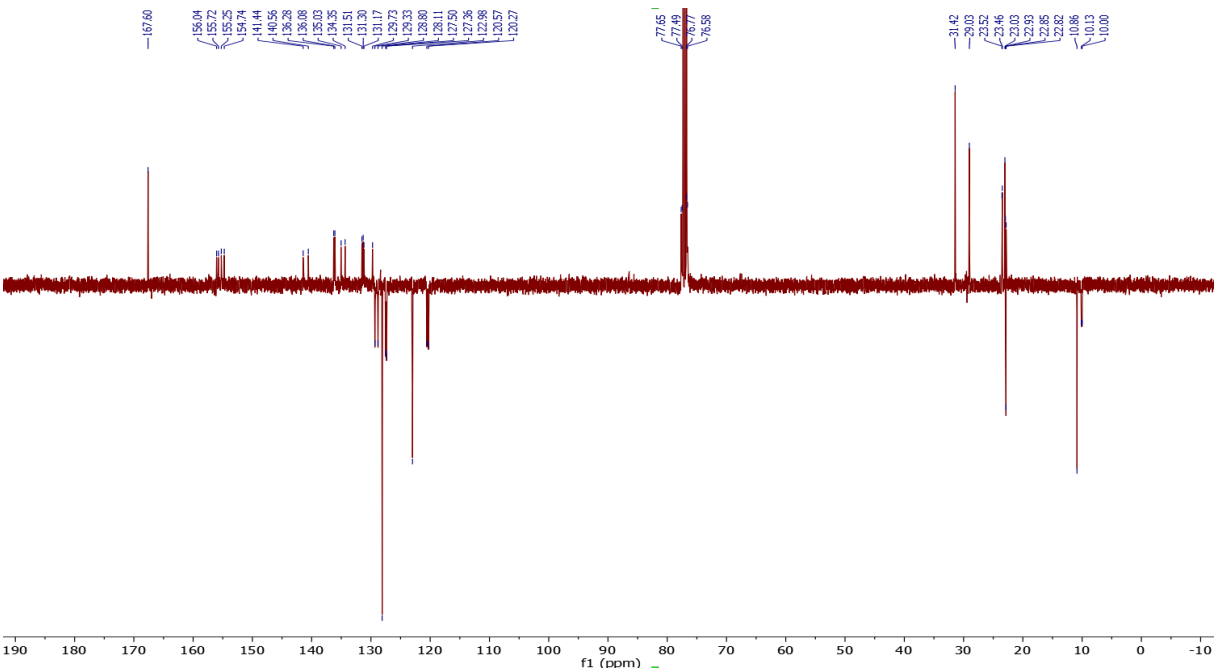

Figure S2: ^{13}C(APT) NMR of compound **7a** ($CDCl_3$, 100 MHz).

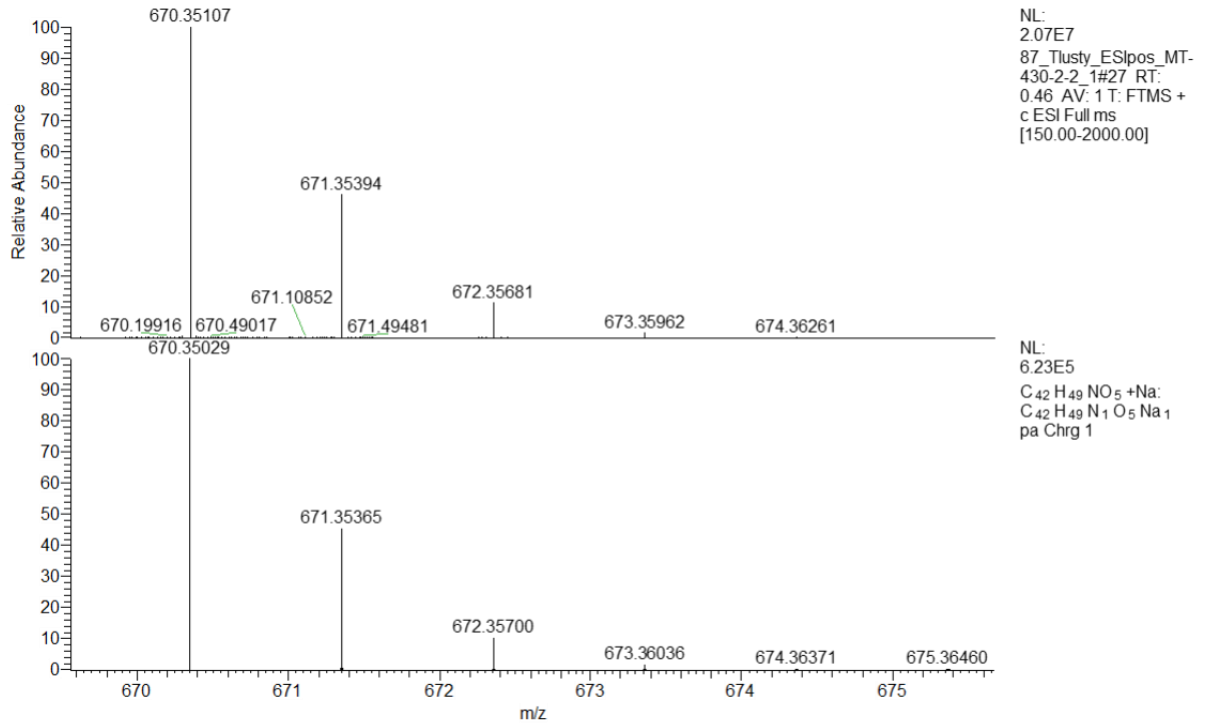

Figure S3: HRMS of compound **7a** (ESI^+).

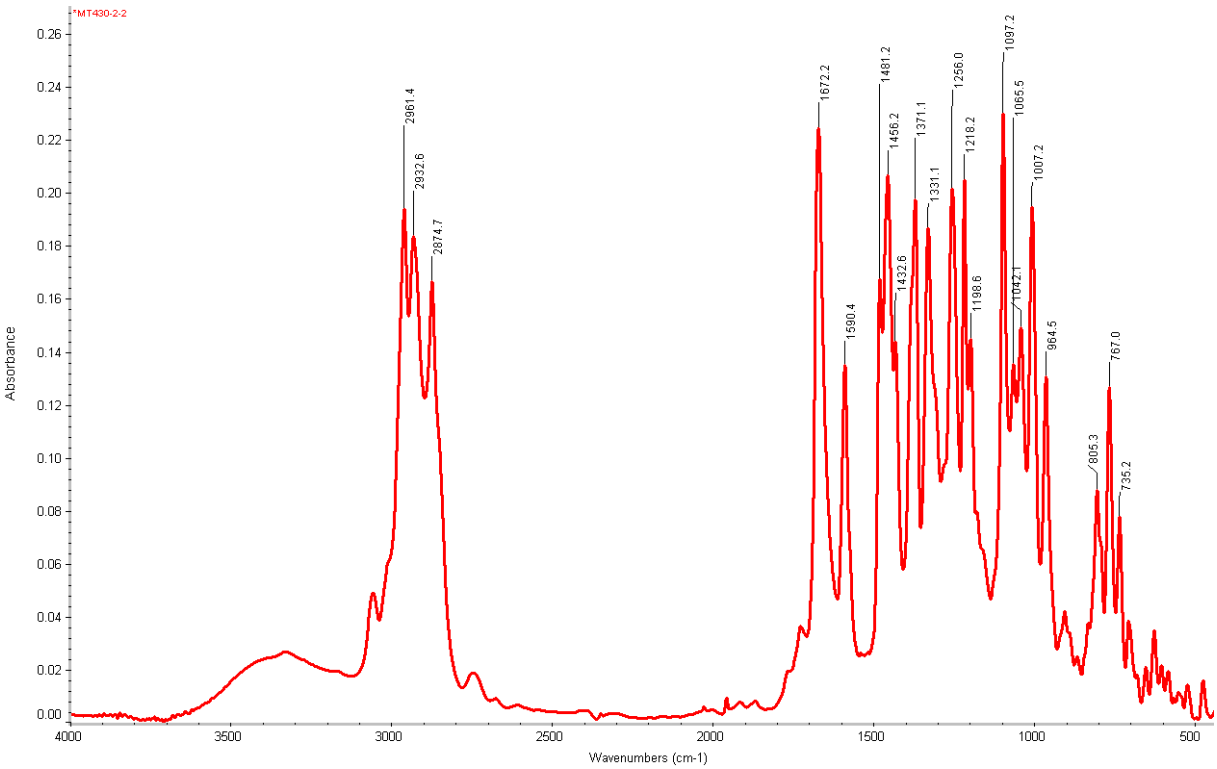

Figure S4: IR of compound **7a** (KBr).

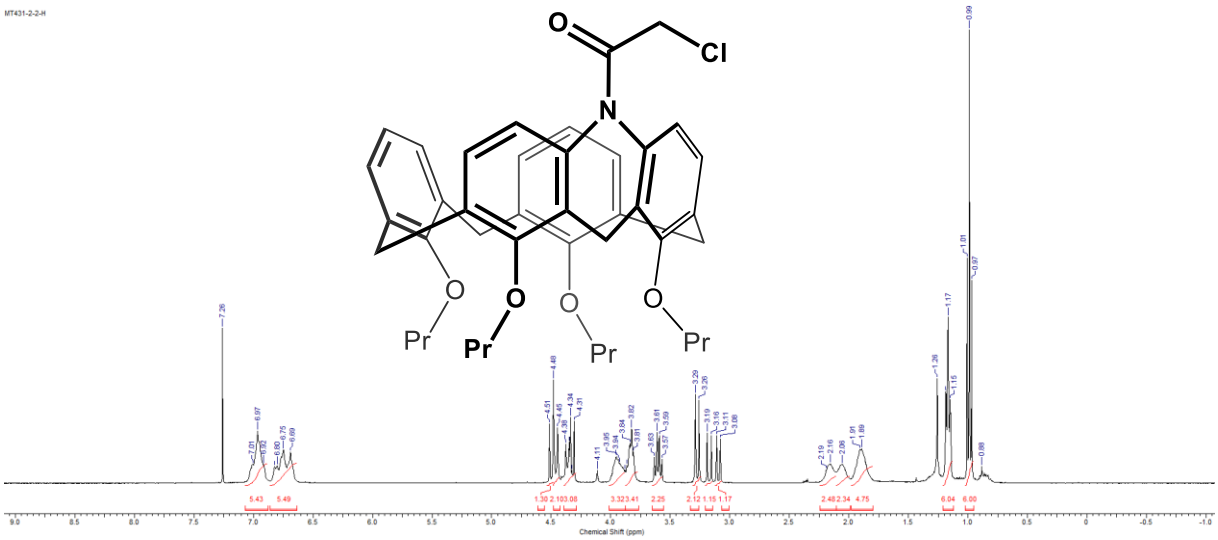

Figure S5: ^{1}H NMR of compound **7b** ($CDCl_3$, 400 MHz).

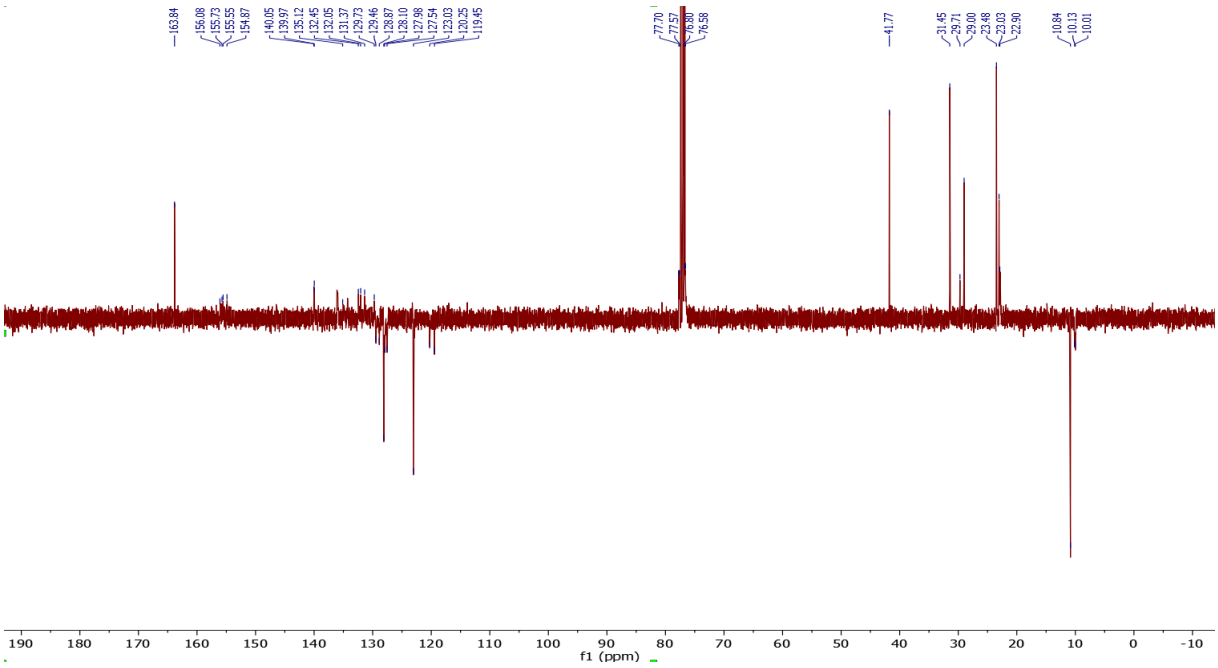

Figure S6: ^{13}C(APT) NMR of compound **7b** ($CDCl_3$, 100 MHz).

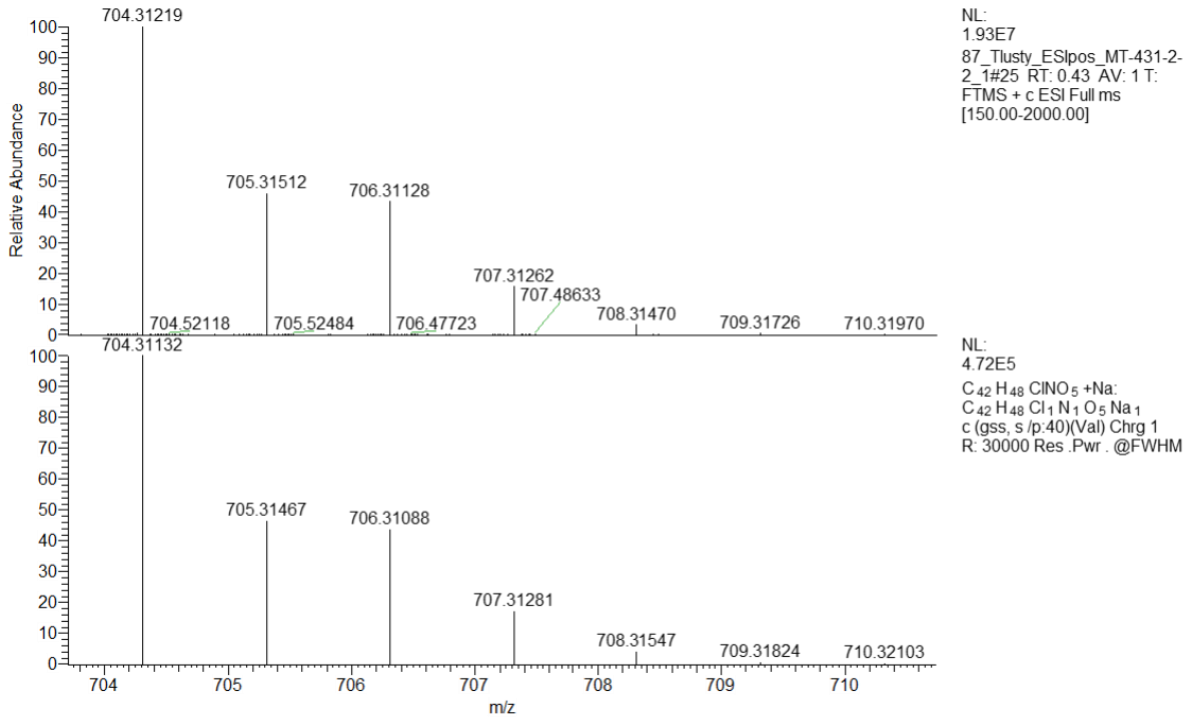

Figure S7: HRMS of compound **7b** (ESI^+).

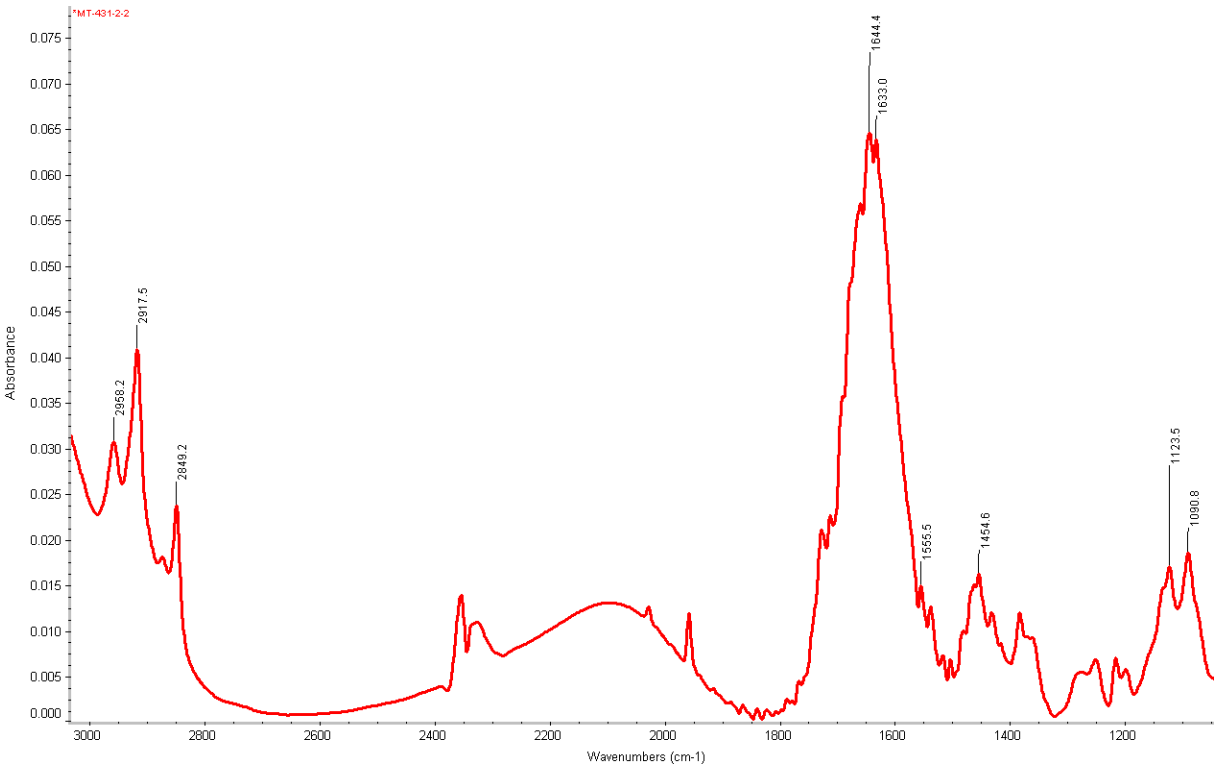

Figure S8: IR of compound **7b** (KBr).

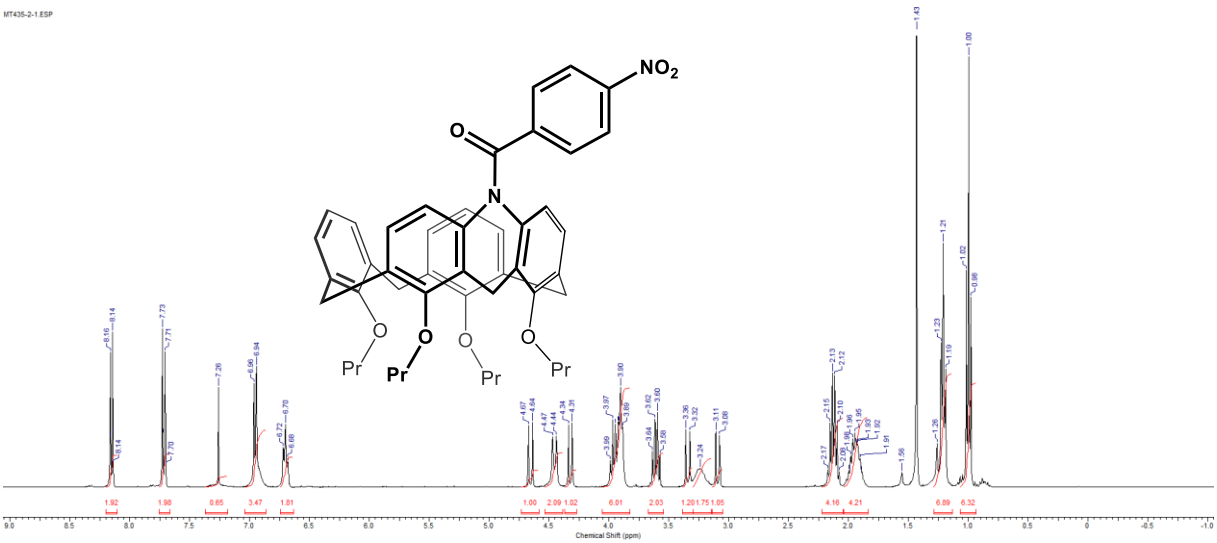

Figure S9: ^{1}H NMR of compound **7c** ($CDCl_3$, 400 MHz).

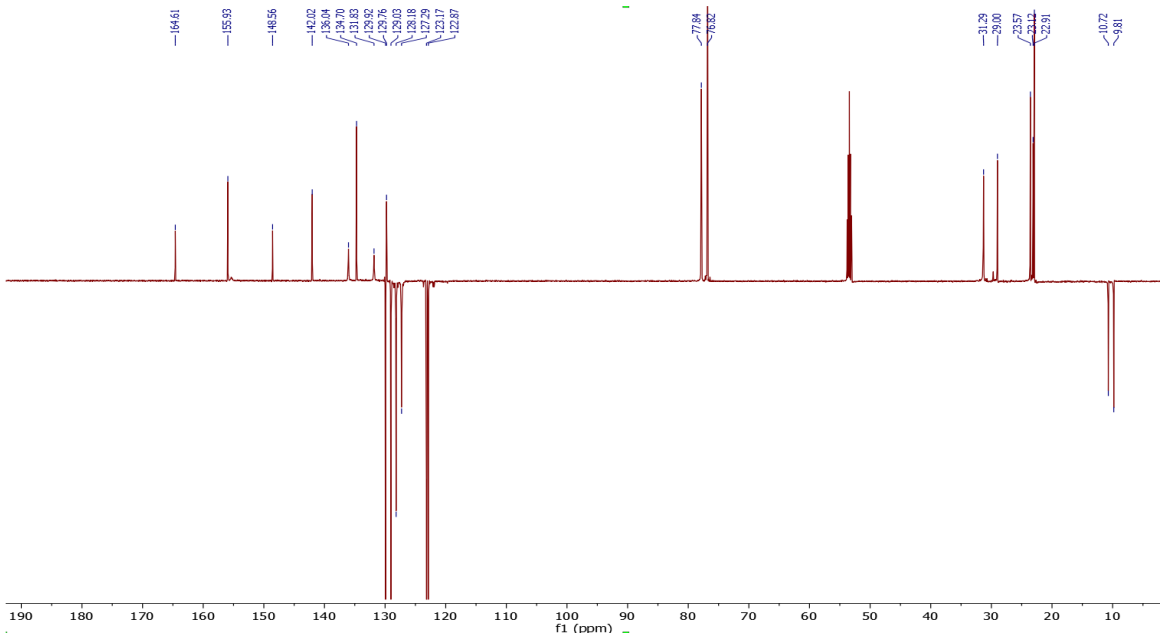

Figure S10: ^{13}C(APT) NMR of compound **7c** ($CDCl_3$, 100 MHz).

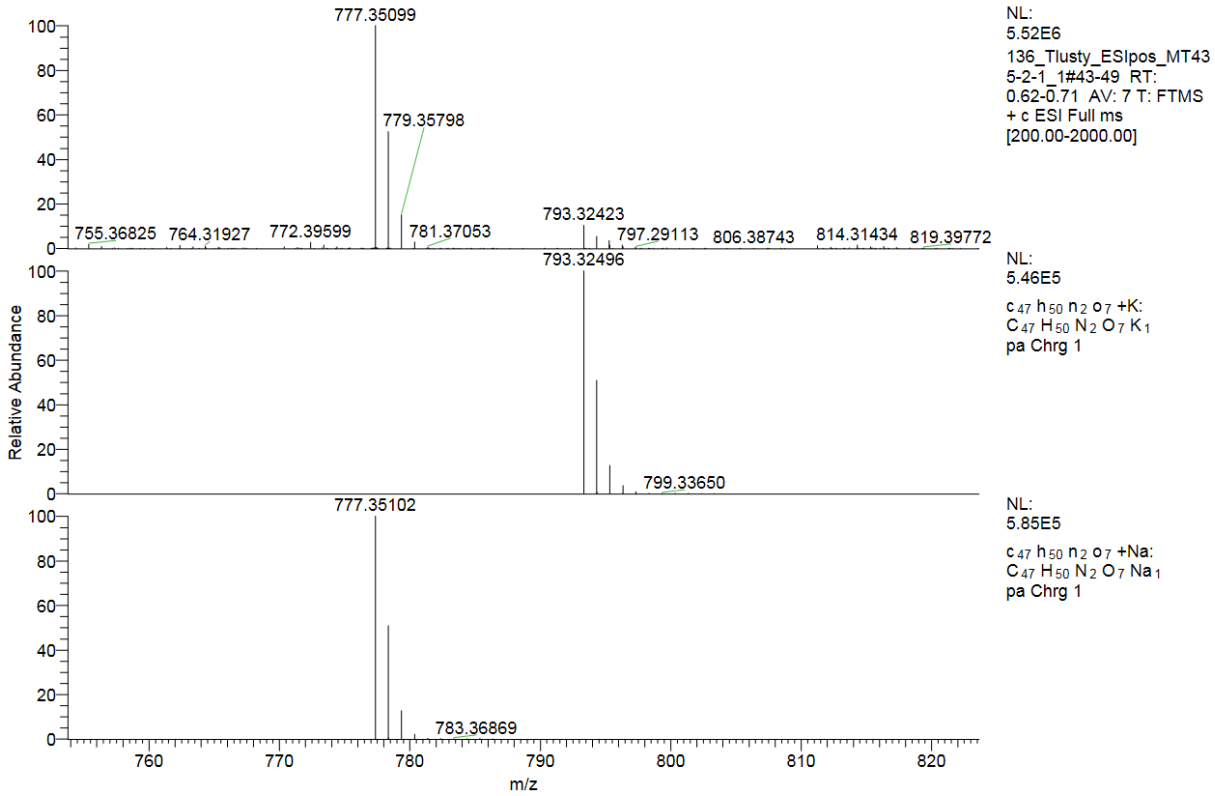

Figure S11: HRMS of compound **7c** (ESI^+).

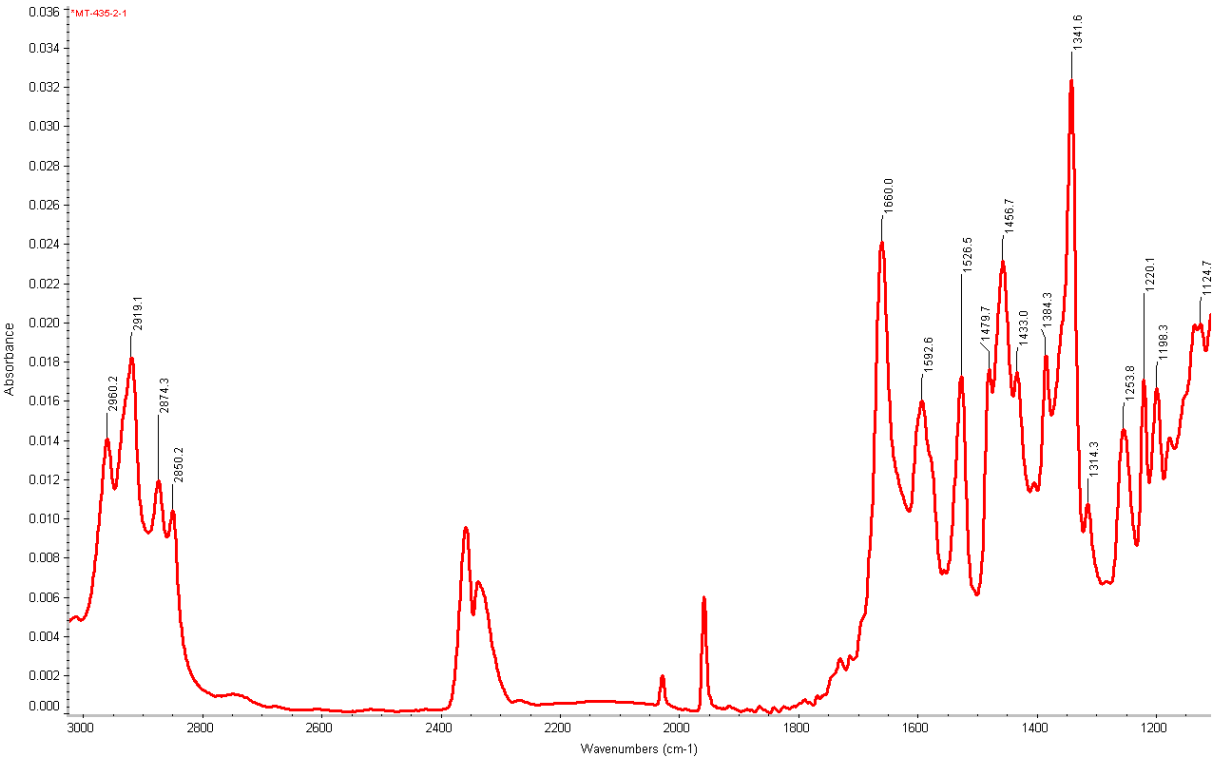

Figure S12: IR of compound **7c** (KBr).

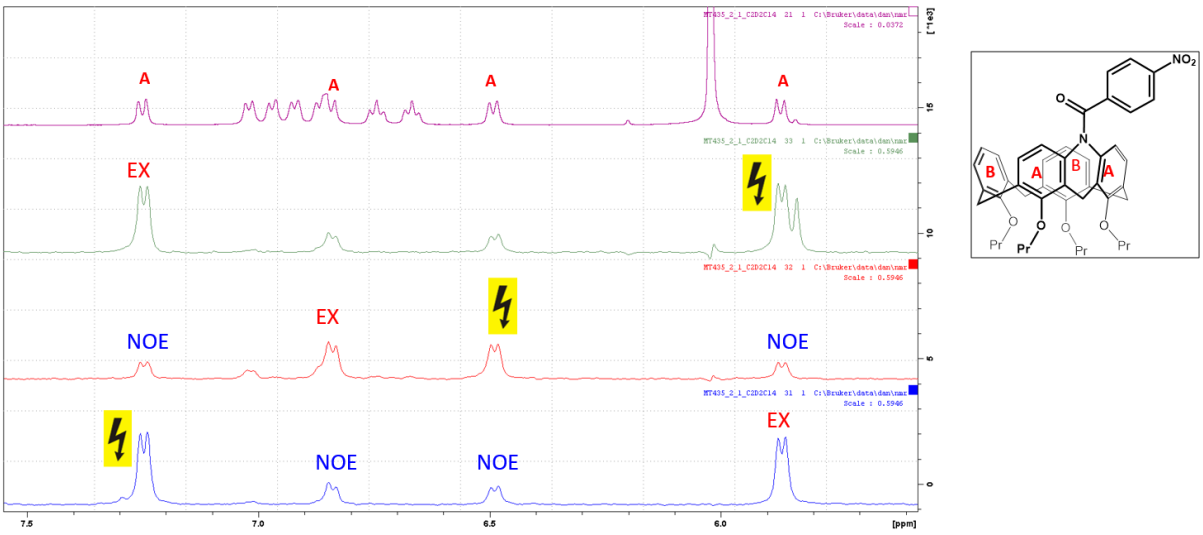

Figure S13: ^{1}H NMR NOE of compound **7c** ($C_2D_2Cl_4$, 253 K, 500 MHz).

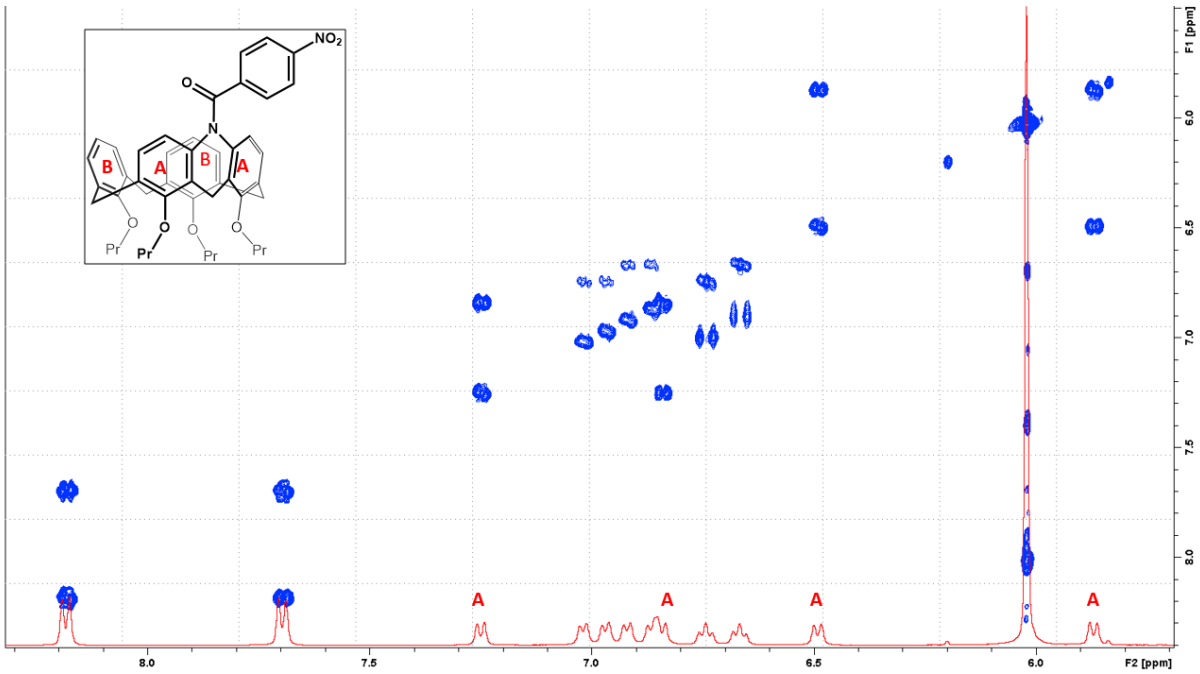

Figure S14: ^{1}H NMR COSY of compound **7c** ($C_2D_2Cl_4$, 253 K, 500 MHz).

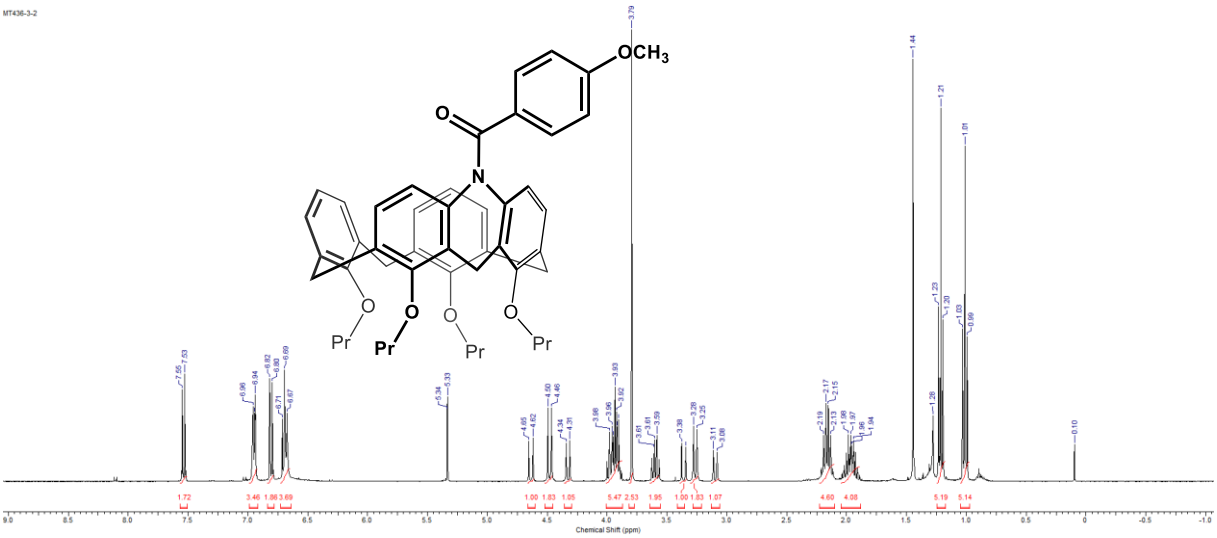

Figure S15: ^{1}H NMR of compound **7d** ($CDCl_3$, 400 MHz).

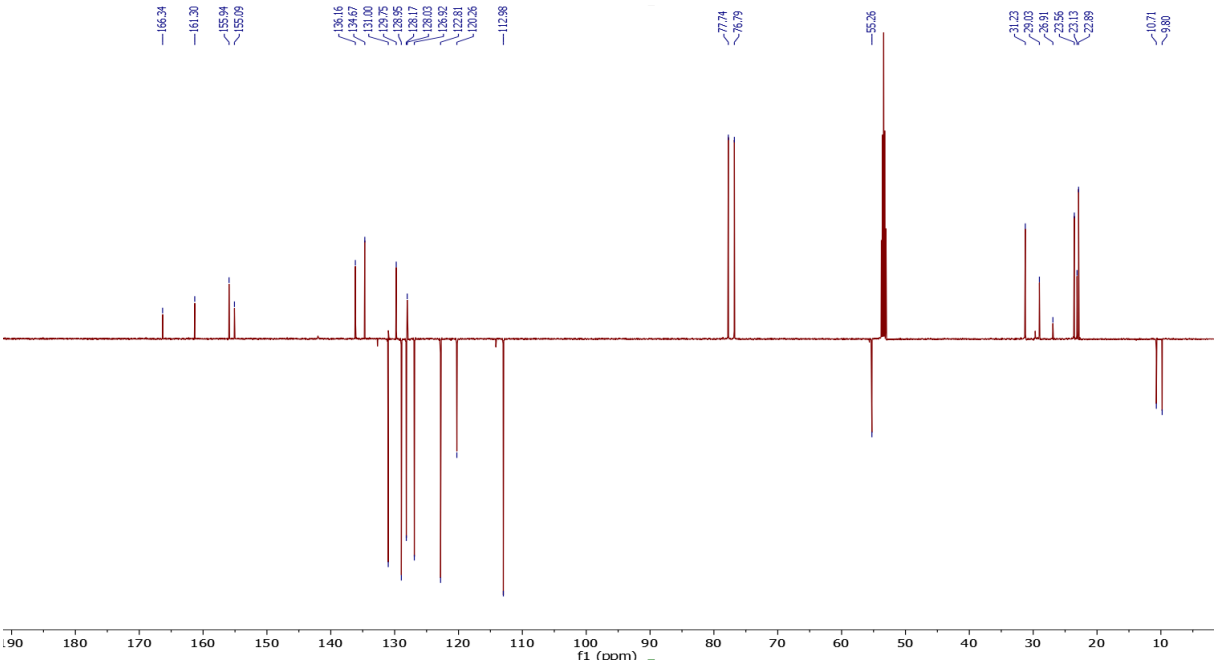

Figure S16: ^{13}C(APT) NMR of compound **7d** ($CDCl_3$, 100 MHz).

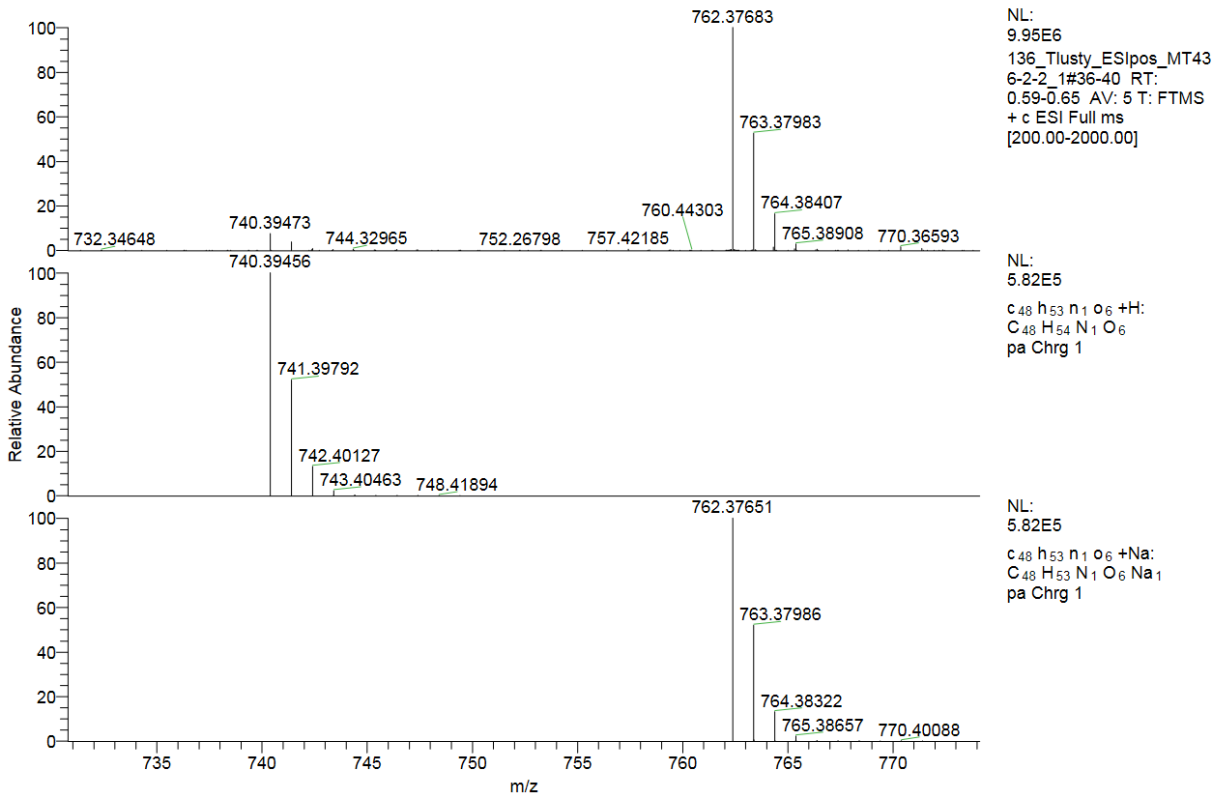

Figure S17: HRMS of compound **7d** (ESI^+).

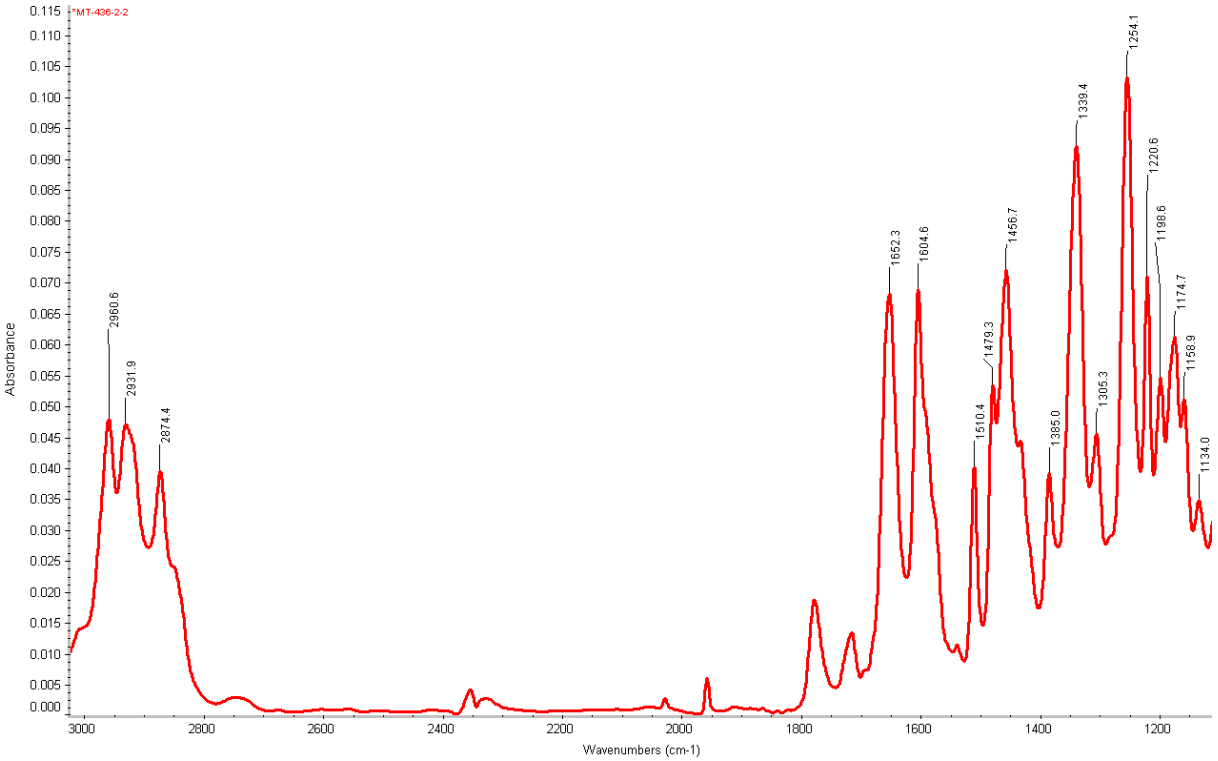

Figure S18: IR of compound **7d** (KBr).

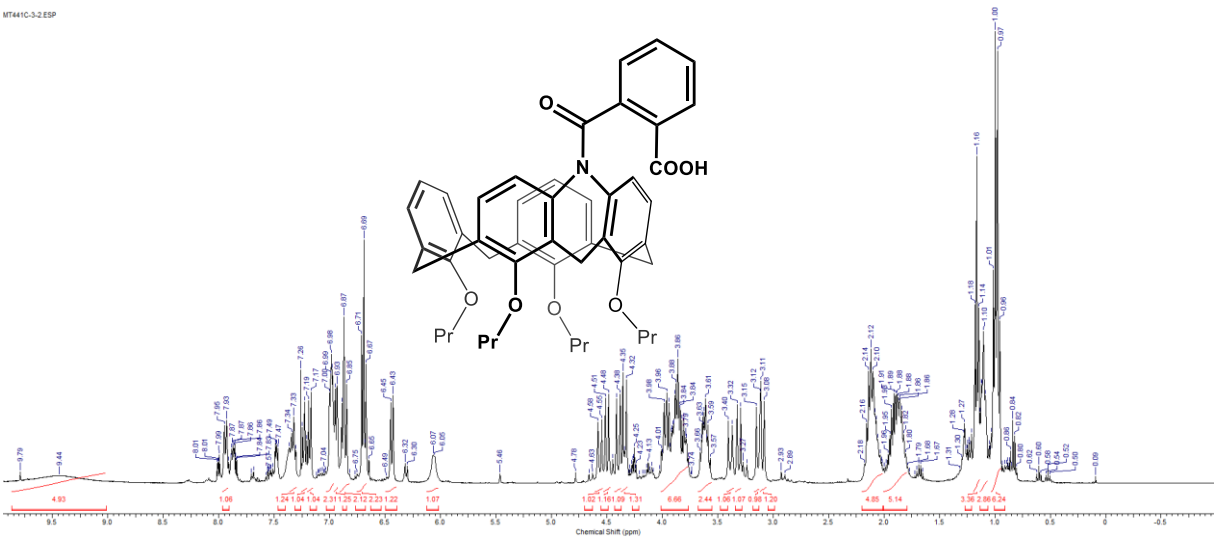

Figure S19: ^{1}H NMR of compound **7e** ($CDCl_3$, 400 MHz).

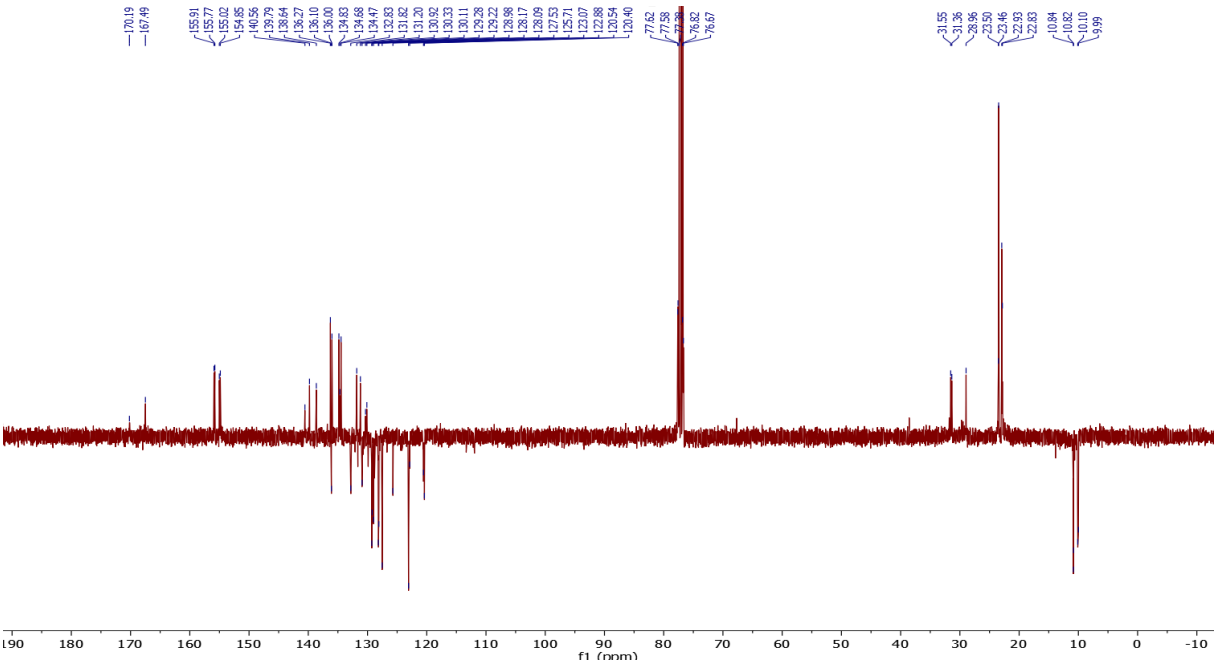

Figure S20: ^{13}C(APT) NMR of compound **7e** ($CDCl_3$, 100 MHz).

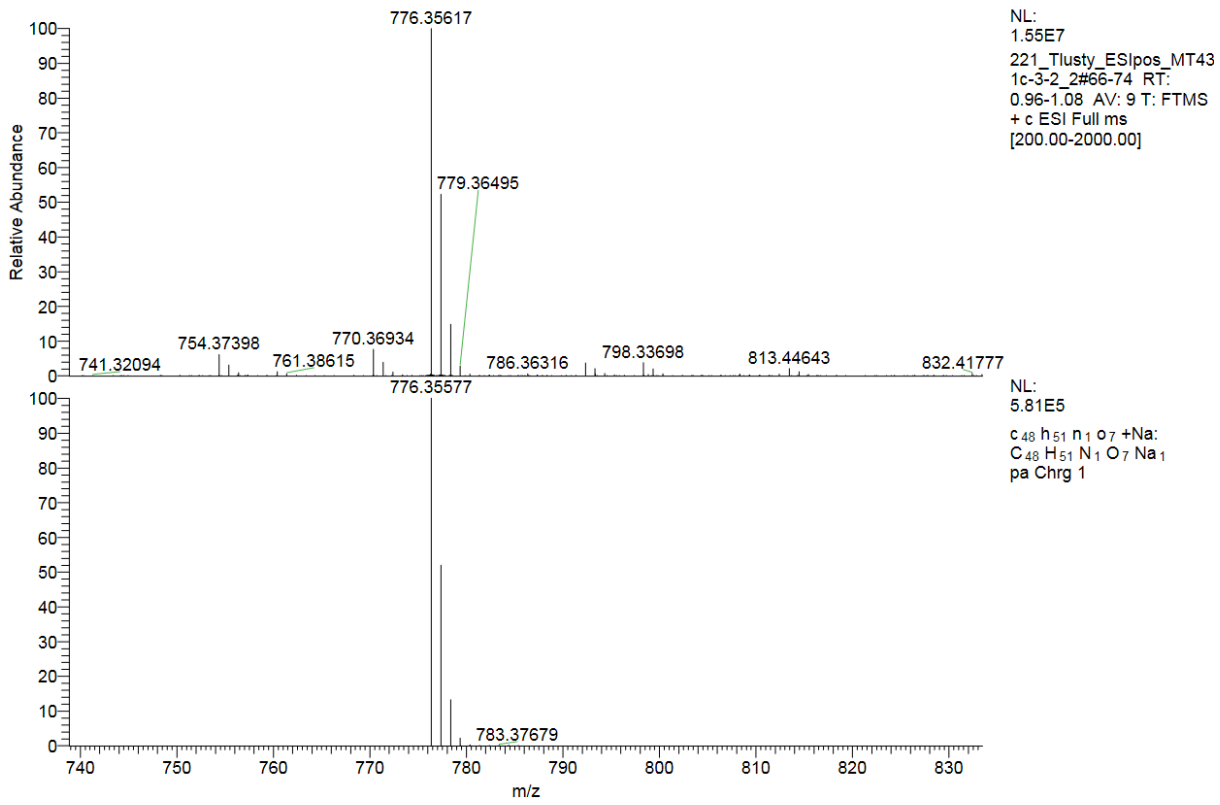

Figure S21: HRMS of compound **7e** (ESI^+).

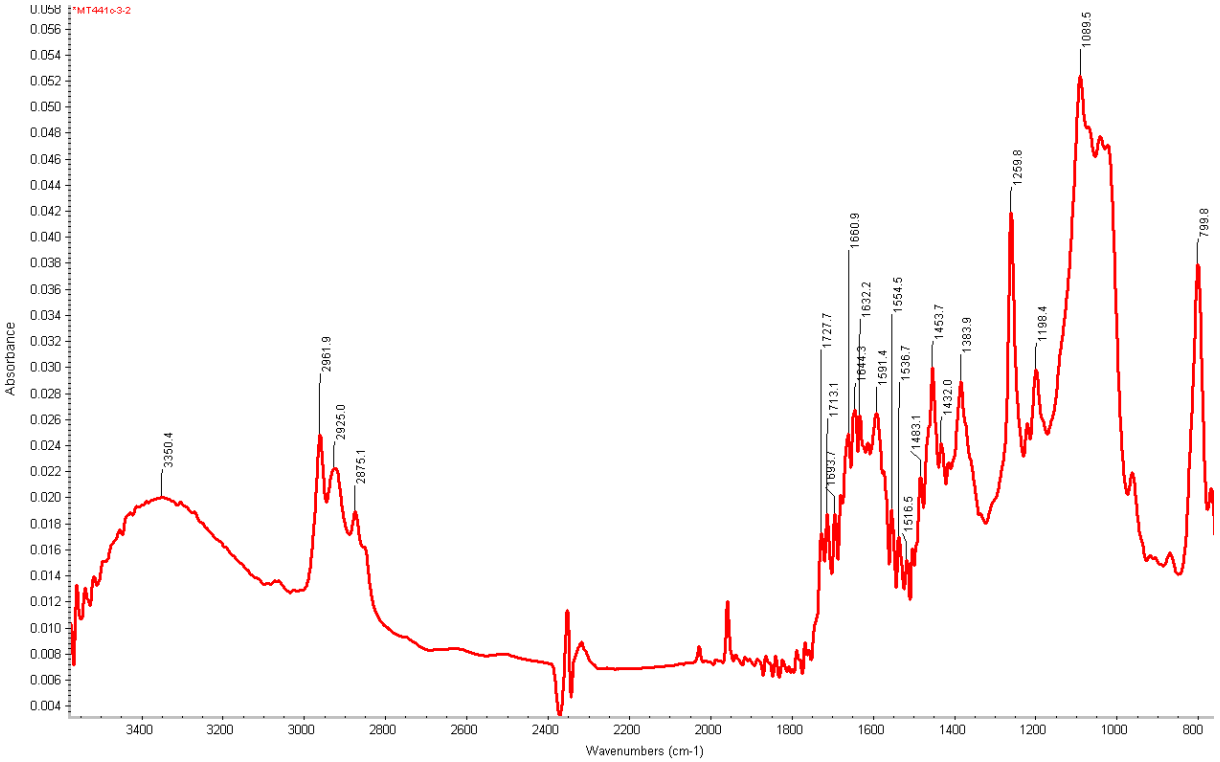

Figure S22: IR of compound **7e** (KBr).

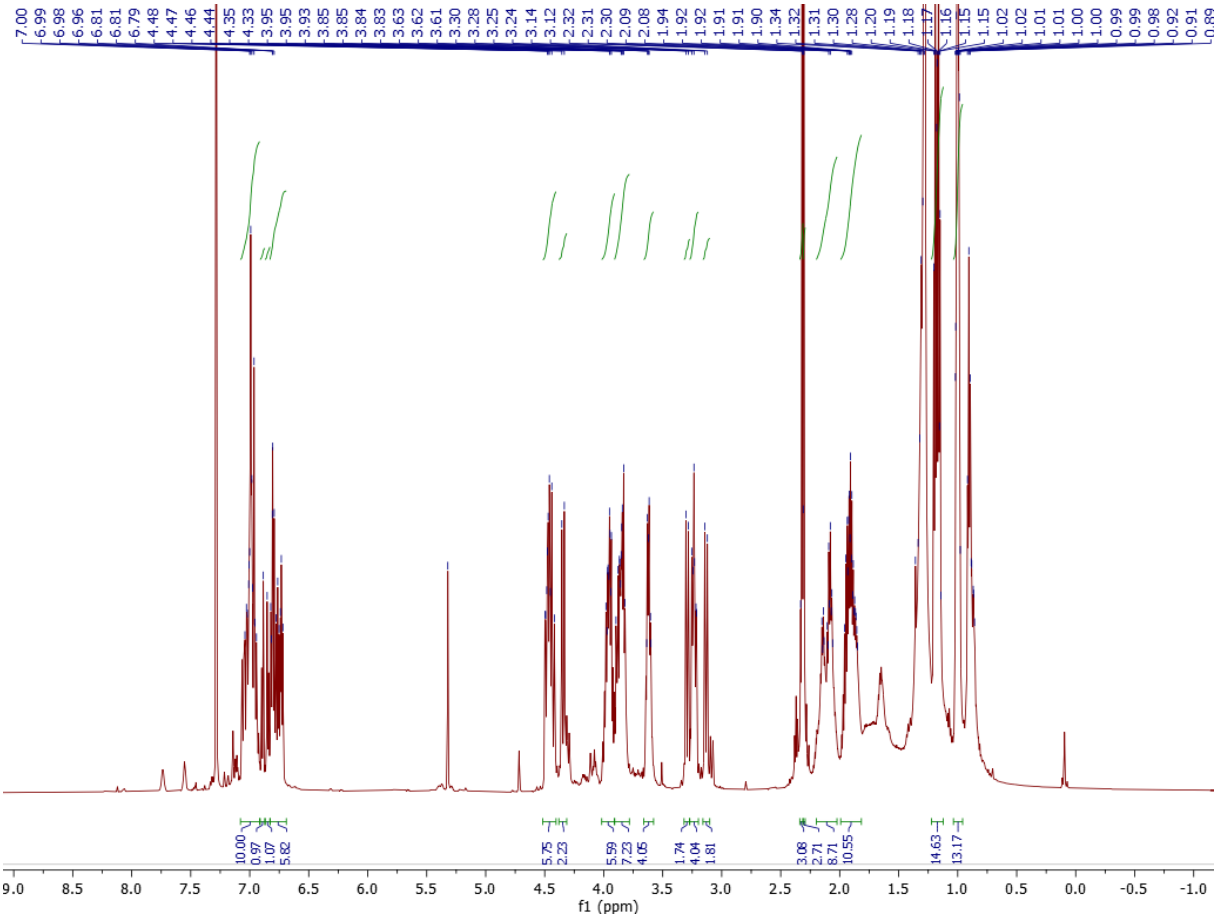

Figure S23: ^{1}H NMR of mixture of compounds **8a** and **8b** ($CDCl_3$, 500 MHz).

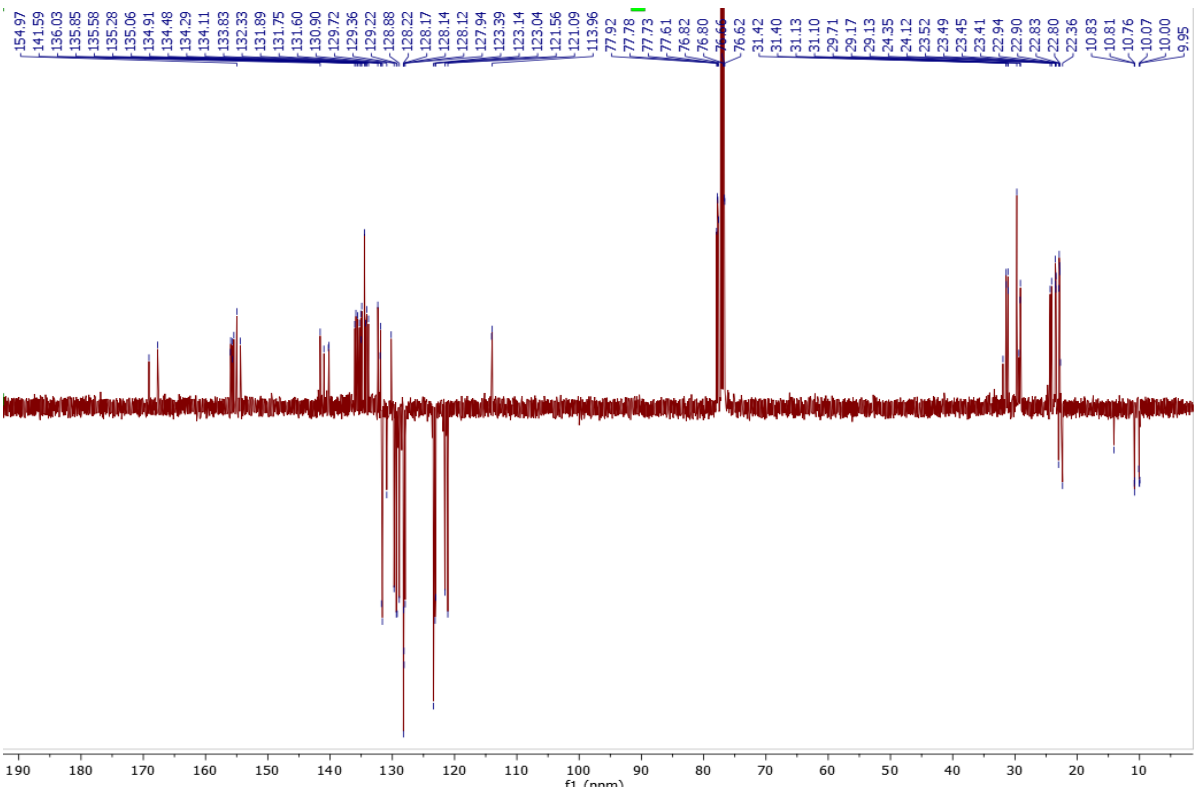

Figure S24: ^{13}C(APT) NMR of mixture of compounds **8a** and **8b** ($CDCl_3$, 125 MHz).

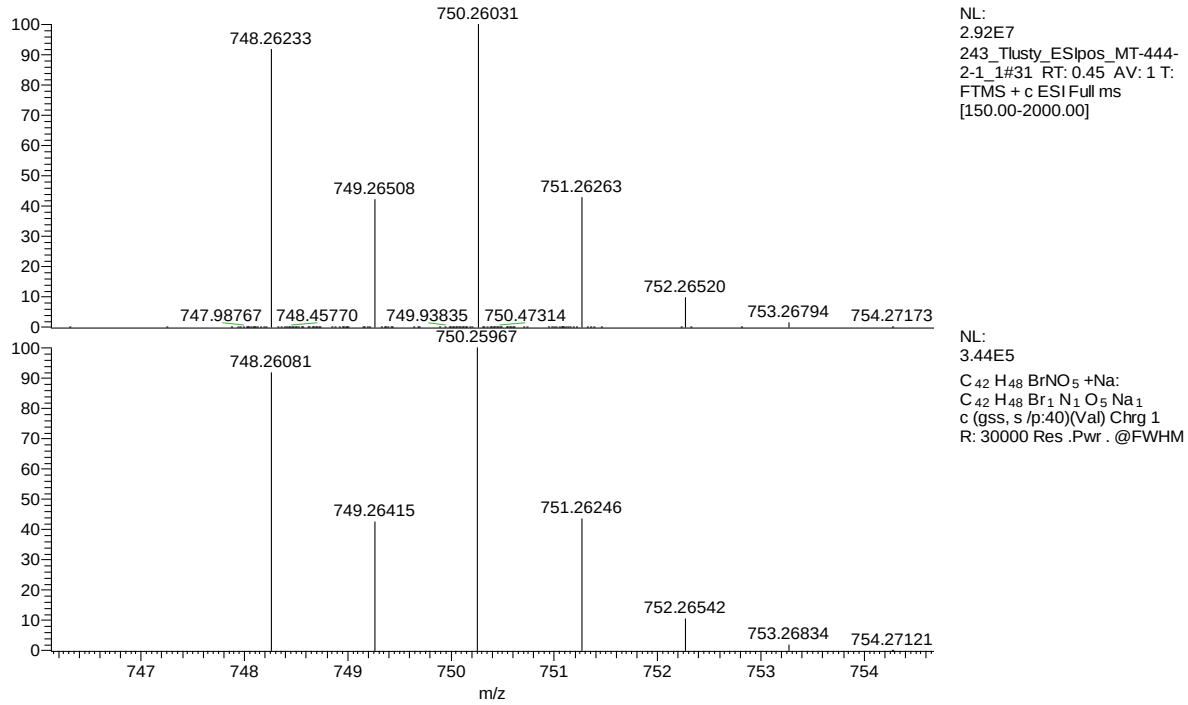

Figure S25: HRMS of mixture of compounds **8a** and **8b** (ESI$^+$).

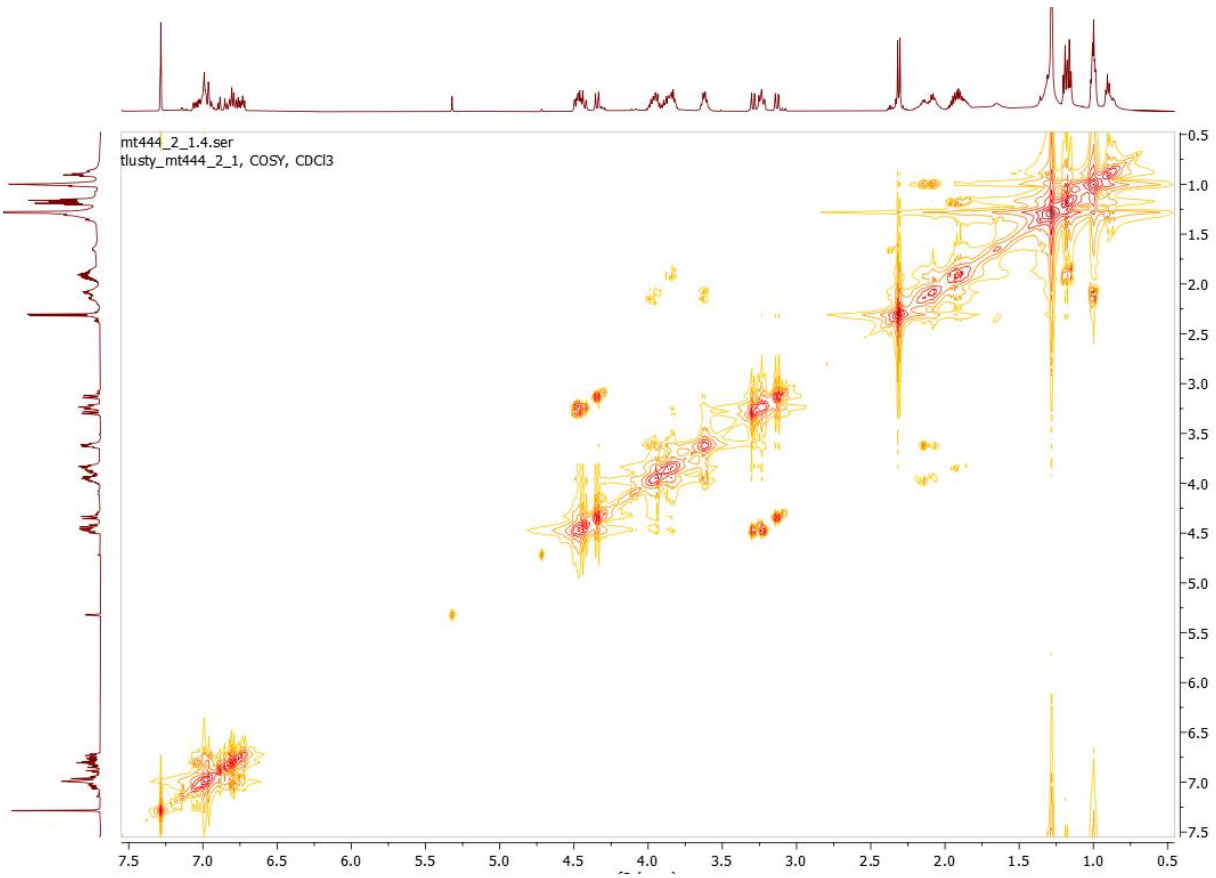

Figure S26: ^{1}H-^{1}H COSY of mixture of compounds **8a** and **8b** ($CDCl_3$, 500 MHz).

Figure S27: ^{1}H-^{1}H COSY (d6 = 200 ms) of mixture of compounds **8a** and **8b** ($CDCl_3$, 500 MHz).

Figure S28: ^{1}H-^{1}H COSY (d6 = 400 ms) of mixture of compounds **8a** and **8b** ($CDCl_3$, 500 MHz).

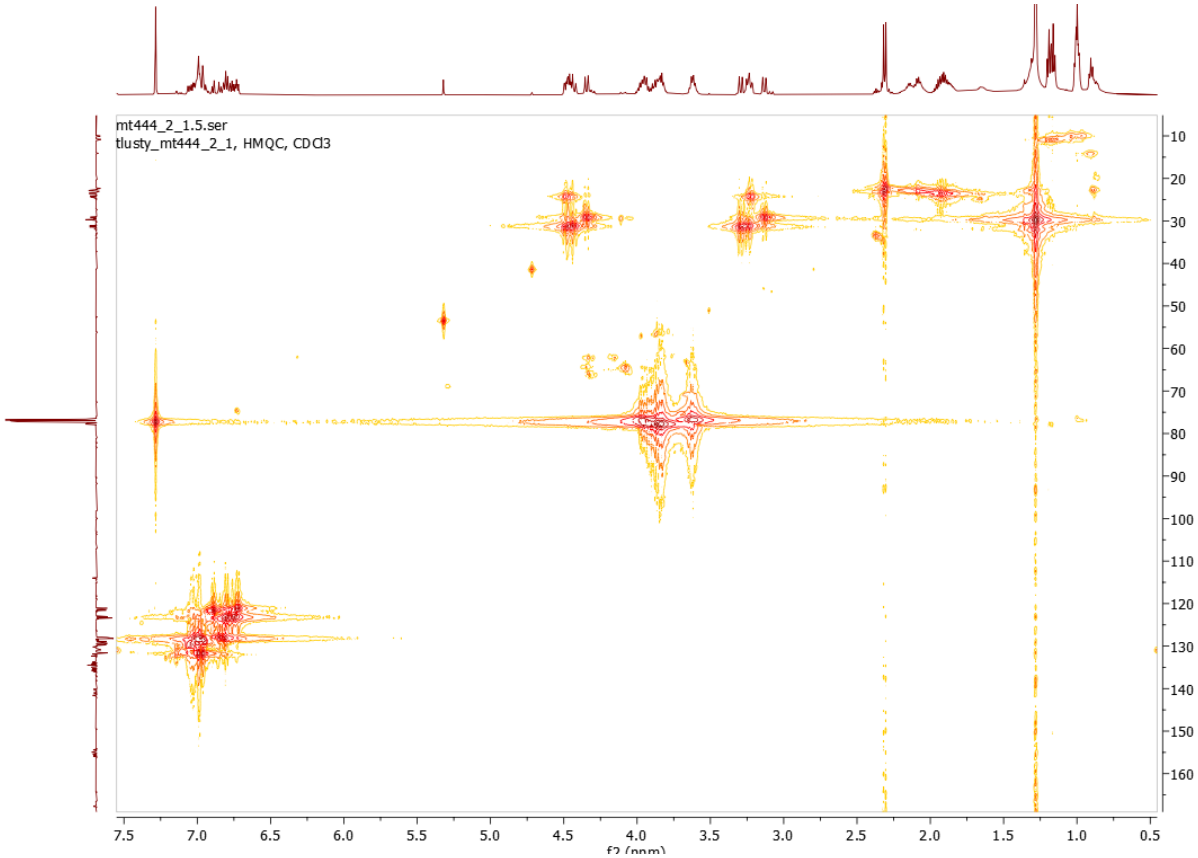

Figure S29: HMQC of mixture of compounds **8a** and **8b** ($CDCl_3$, 500, 125 MHz).

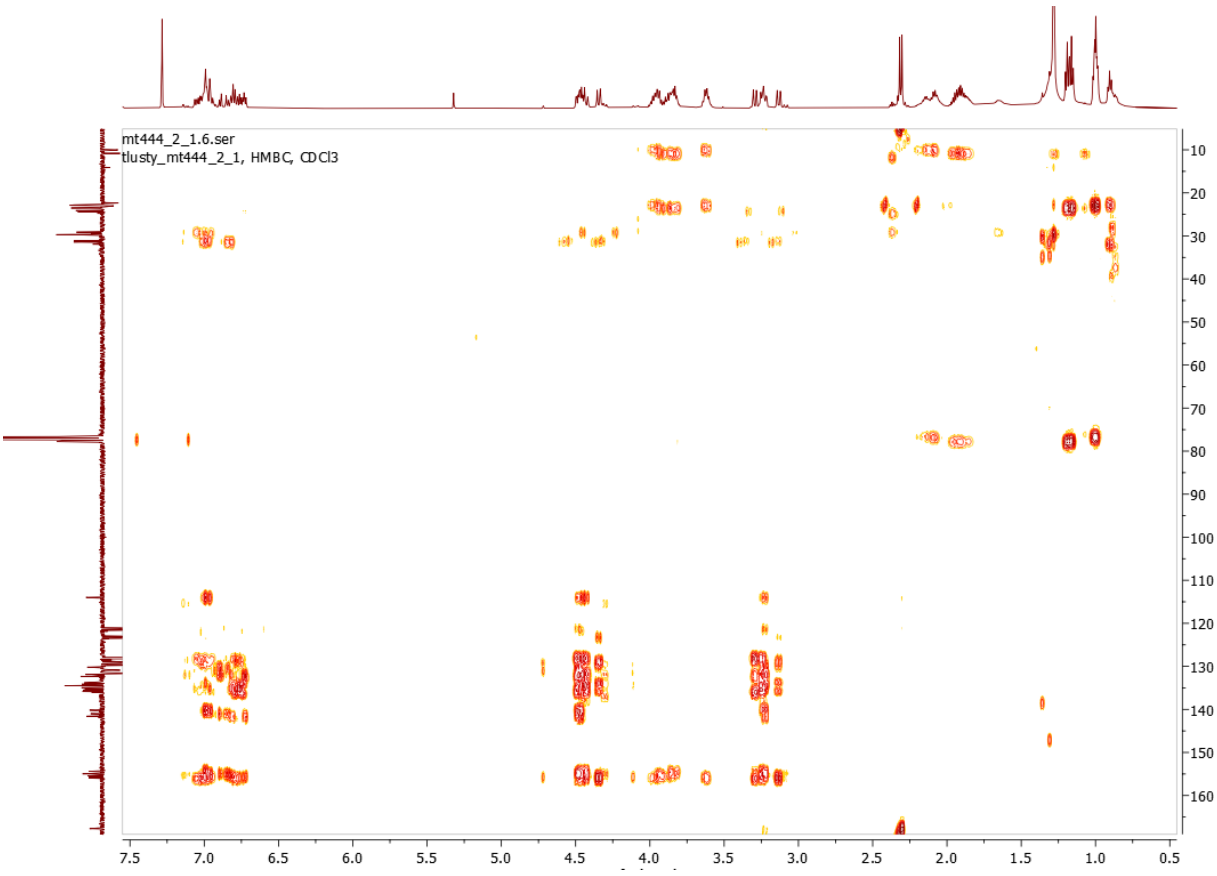

Figure S30: HMBC of mixture of compounds **8a** and **8b** ($CDCl_3$, 500, 125 MHz).

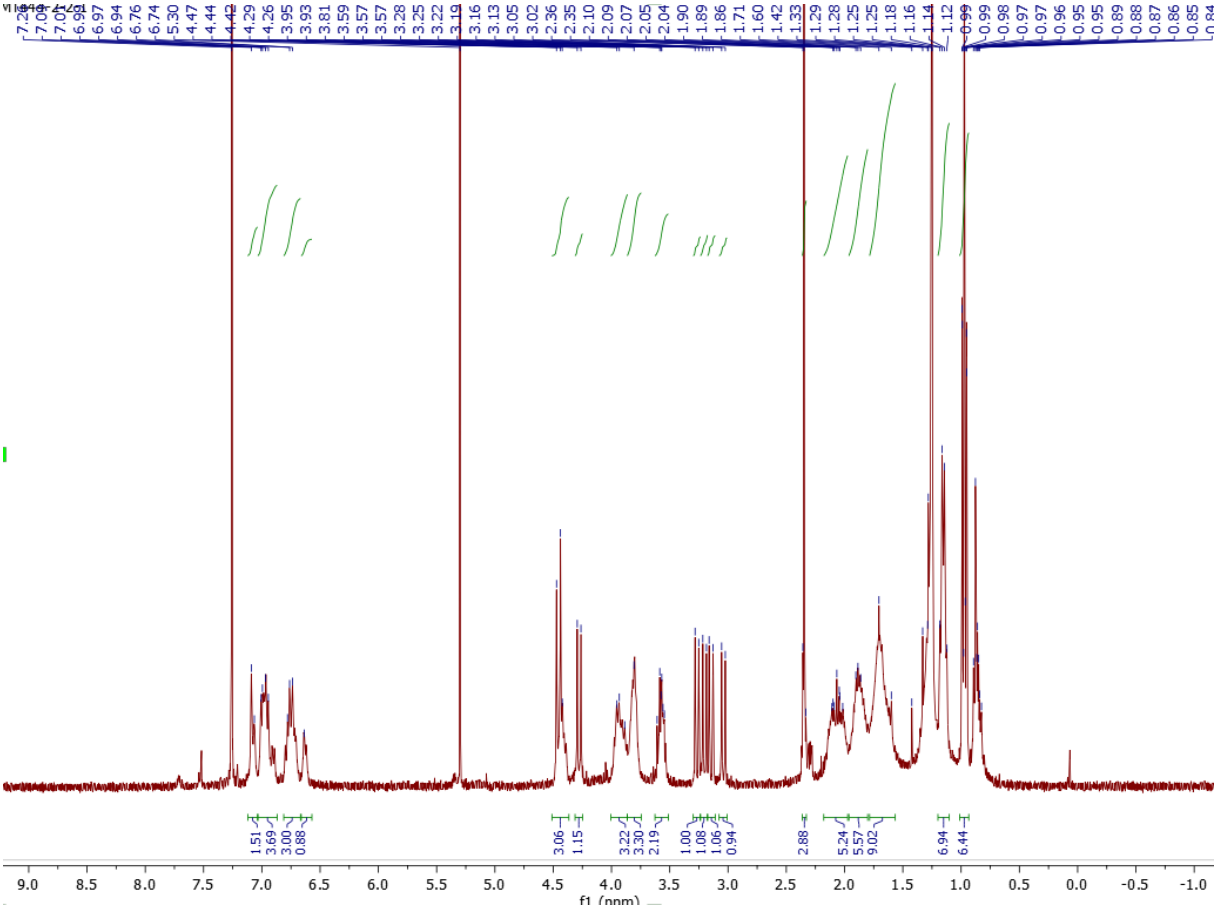

Figure S31: ^{1}H NMR of mixture of compounds **8c** ($CDCl_3$, 500 MHz).

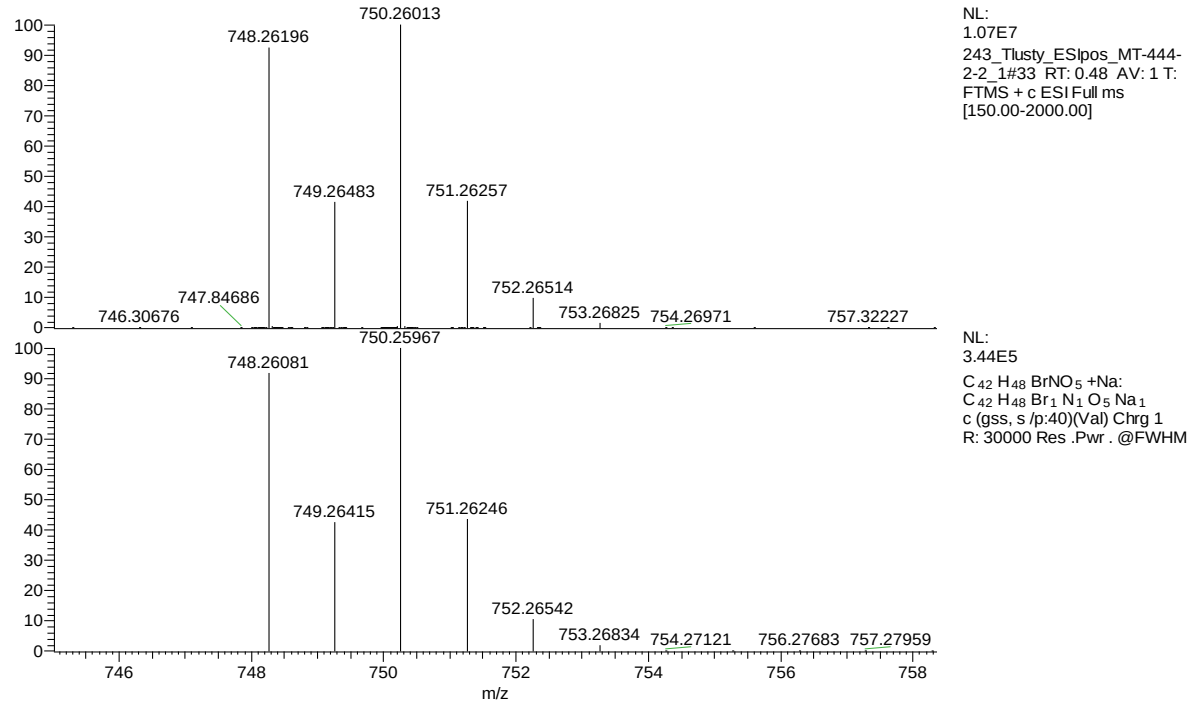

Figure S32: HRMS of compound **8c** (ESI^+).

2. Dynamic NMR measurements

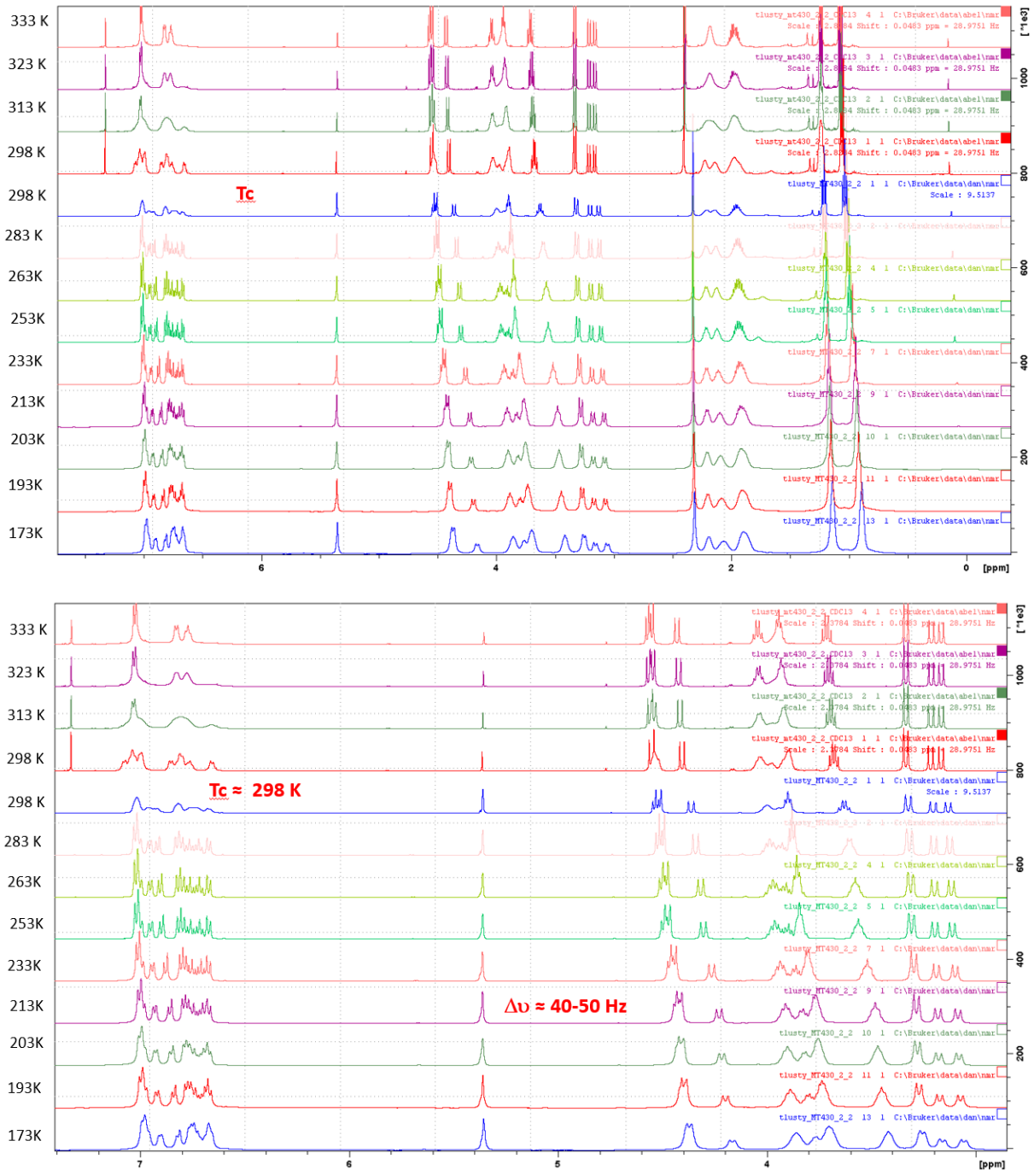

Figure S33: Temperature-dependent ^{1}H NMR spectra of **7a** (333 – 298 K: $CDCl_3$, 298 – 173 K: CD_2Cl_2, 500 MHz)

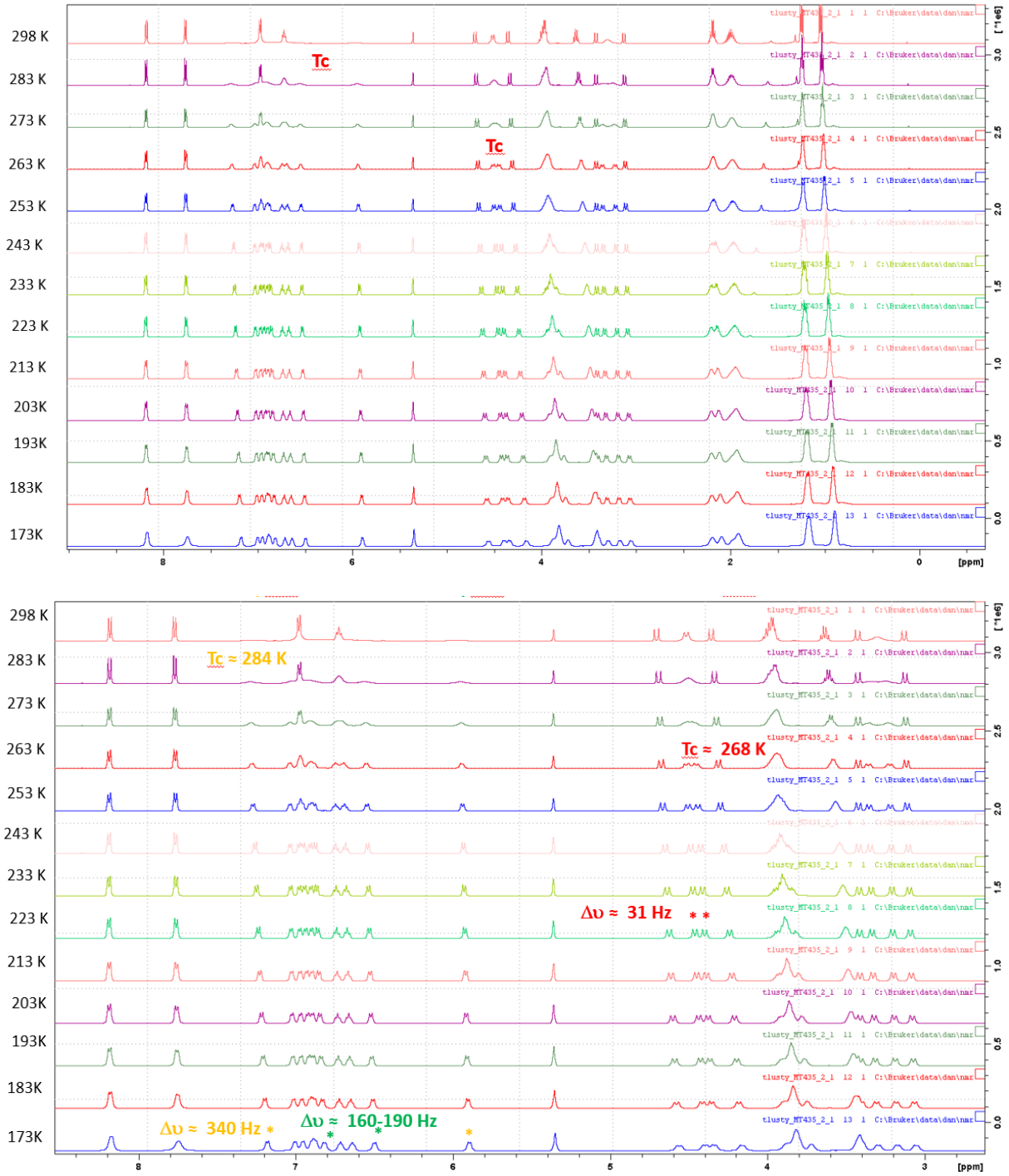

Figure S34: Temperature-dependent ^{1}H NMR spectra of **7c** (298 – 173 K: CD_2Cl_2, 500 MHz)

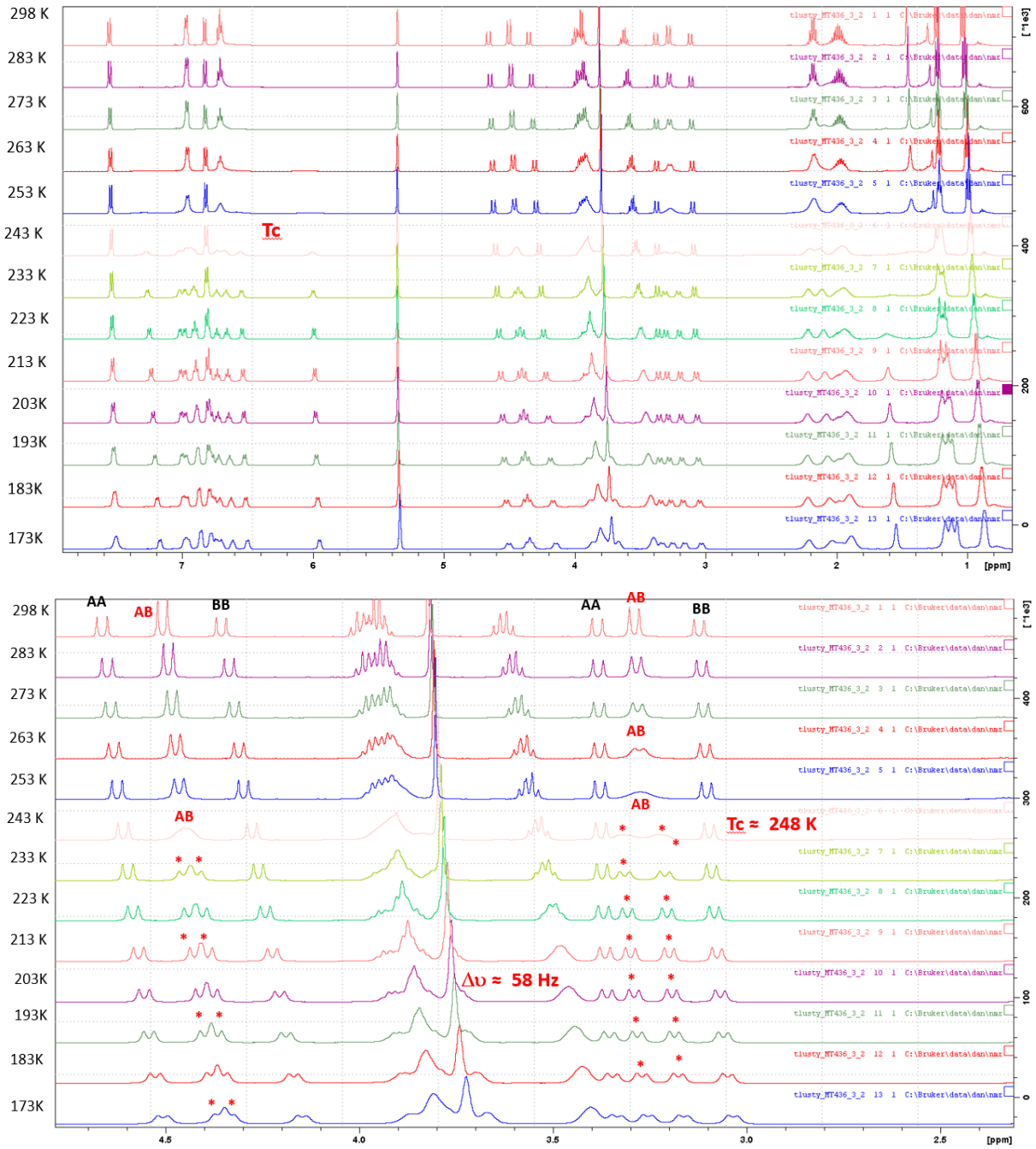

Figure S35: Temperature-dependent ^{1}H NMR spectra of **7d** (298 – 173 K: CD_2Cl_2, 500 MHz)

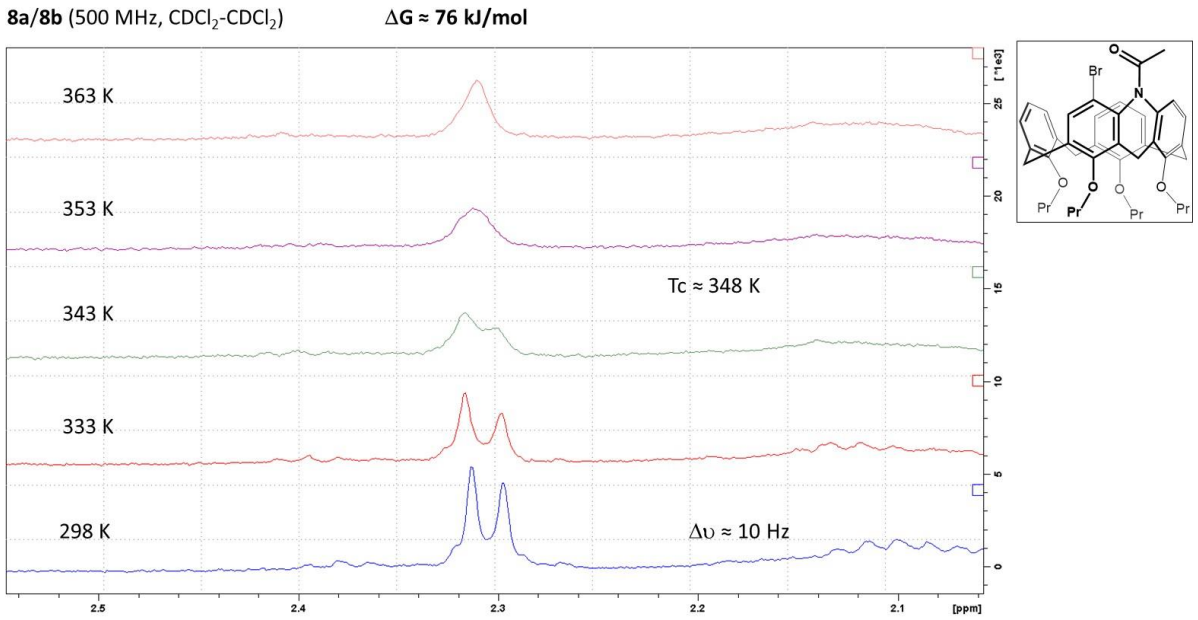

Figure S36: Temperature-dependent ^{1}H NMR spectra of **8a/8b** (298 – 363 K: $CDCl_2$-$CDCl_2$, 500 MHz)

3. Crystallographic data

Crystallographic data for **7c**

M = 754.92 g.mol^{-1}, monoclinic system, space group $P2_1/c$, a = 9.46594 (8) Å, b = 17.66158 (14) Å, c = 23.8239 (2) Å, β = 90.2849 (7)°, Z = 4, V = 3982.91 (6) Å^3, D_c = 1.259 g.cm^{-3}, μ(Cu-Kα) = 0.68 mm^{-1}, crystal dimensions of 0.49 × 0.16 × 0.09 mm. Data were collected at 130 (2) K on a Rigaku OD Gemini AtlasS2 CCD diffractometer with mirror collimated sealed X-ray tube Cu-Kα radiation. The structure was solved by charge flipping methods[1] and anisotropically refined by full matrix least squares on F squared using the CRYSTALS suite of programs[2] to final value R = 0.037 and wR = 0.095 using 7139 independent reflections (θ_{max} = 67.7°), 563 parameters and 58 restrains. The hydrogen atoms bonded to carbon atoms were placed in calculated positions refined with a riding constrains. The disordered functional groups positions were found in difference electron density maps and refined with restrained geometry. MCE[3] was used for visualization of electron density maps. The occupancy of disordered functional group was constrained to full. The structure was deposited into Cambridge Structural Database under number CCDC 2157472.

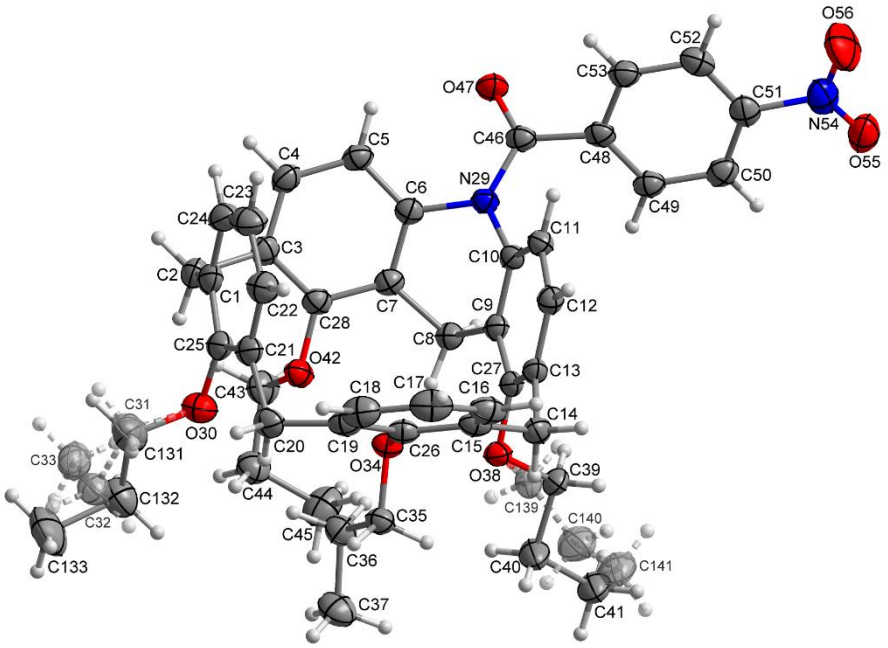

Figure S37: The asymmetric unit of crystal structure **7c**, the ADPs drawn at 50% probability level. The weakly occupied atoms depicted as transparent.

[1] Palatinus, L., Chapuis, G. (2007). J. Appl. Cryst. 40, 786-790.

[2] Betteridge, P.W., Carruthers, J.R., Cooper, R.I., Prout, K. & Watkin, D.J. (2003). J. Appl. Cryst. 36, 1487.

[3] Rohlicek J., Husak M.: J. Appl. Cryst. 40, 600 (2007)

4. Titration experiments

Calixarene **7c** was dissolved in a specified amount of $C_2D_2Cl_4$. 0.5 ml of calixarene solution was put in an NMR tube. To the calixarene solution (0.6 ml), a specific amount of *N*-methylisoquinolinium iodide (NMII) was added. The aliquots of NMII were gradually added to the NMR tube to achieve different calixarene/guest ratios (1:0.000-50.012), ensuring constant host concentration during the experiment. The complexation constant was determined by analyzing CIS of host protons using nonlinear curve-fitting procedure (program BindFit).

M(NMII)	271,10147	g/mol	M(calix)	754,924	g/mol
m(NMII)	0,00859	g	m(calix)	0,00200	g
c(NMII)	0,05281	mol/l	c(calix)	0,00053	mol/l
V(C2D2Cl4_NMII)	0,6	ml	V(C2D2Cl4_cali	5	ml

	V (total) [m	V(addition, total) [n	V(addition) [ml]	c(NMII) [mol/l]	c(calix) [mol/l]	c(calix)/c(NM	shift [Hz]
1	0,5000	0,0000	0,0000	0,00000	0,00053	0,00000	3276,67
2	0,5006	0,0006	0,0006	0,00006	0,00053	0,11946	3276,87
3	0,5012	0,0012	0,0006	0,00013	0,00053	0,23863	3276,67
4	0,5020	0,0020	0,0008	0,00021	0,00053	0,39708	3276,97
5	0,5028	0,0028	0,0008	0,00029	0,00053	0,55503	3276,77
6	0,5042	0,0042	0,0014	0,00044	0,00053	0,83023	3277,07
7	0,5056	0,0056	0,0014	0,00058	0,00053	1,10391	3277,16
8	0,5136	0,0136	0,0080	0,00140	0,00053	2,63917	3276,77
9	0,5236	0,0236	0,0100	0,00238	0,00053	4,49227	3275,89
10	0,5536	0,0536	0,0300	0,00511	0,00053	9,64988	3275,31
11	0,5936	0,0936	0,0400	0,00833	0,00053	15,71575	3274,33
12	0,6436	0,1436	0,0500	0,01178	0,00053	22,23779	3274,33
13	0,7136	0,2136	0,0700	0,01581	0,00053	29,83319	3273,45
14	0,8036	0,3036	0,0900	0,01995	0,00053	37,65435	3273,06
15	0,9036	0,4036	0,1000	0,02359	0,00053	44,51724	3271,88
16	1,0036	0,5036	0,1000	0,02650	0,00053	50,01248	3271,10

K	3,86 M^{-1}
Error	0,34844606 M^{-1}

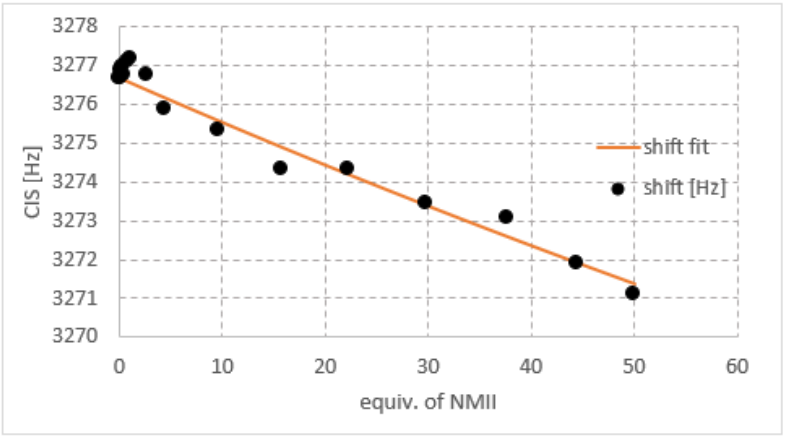

Figure S38: ^{1}H NMR titration of compound **7c** with NMII ($C_2D_2Cl_4$, 400 MHz).

Calixarene **7c** was dissolved in a specified amount of $C_2D_2Cl_4$. 0.5 ml of calixarene solution was put in an NMR tube. To the calixarene solution (0.6 ml), a specific amount of *N*-methylpyridinium iodide (NMPI) was added. The aliquots of NMPI were gradually added to the NMR tube to achieve different calixarene/guest ratios (1:0.000-46.843), ensuring constant host concentration during the experiment. The complexation constant was determined by analyzing CIS of host protons using nonlinear curve-fitting procedure (program BindFit).

M(NMPI)	221,04147 g/mol	M(calix)	754,924 g/mol
m(NMPI)	0,00656 g	m(calix)	0,00200 g
c(NMPI)	0,04946 mol/l	c(calix)	0,00053 mol/l
V(C2D2Cl4_NMPI)	0,6 ml	V(C2D2Cl4_cali	5 ml

	V (total) [m	V(addition, total) [n	V(addition) [ml]	c(NMPI) [mol/l]	c(calix) [mol/l]	c(calix)/c(NM	shift [Hz]
1	0,5000	0,0000	0,0000	0,00000	0,00053	0,00000	3269,44
2	0,5006	0,0006	0,0006	0,00006	0,00053	0,11189	3269,24
3	0,5012	0,0012	0,0006	0,00012	0,00053	0,22351	3268,95
4	0,5020	0,0020	0,0008	0,00020	0,00053	0,37192	3268,46
5	0,5028	0,0028	0,0008	0,00028	0,00053	0,51986	3269,05
6	0,5042	0,0042	0,0014	0,00041	0,00053	0,77762	3270,02
7	0,5056	0,0056	0,0014	0,00055	0,00053	1,03396	3269,44
8	0,5136	0,0136	0,0080	0,00131	0,00053	2,47193	3268,85
9	0,5236	0,0236	0,0100	0,00223	0,00053	4,20760	3267,97
10	0,5536	0,0536	0,0300	0,00479	0,00053	9,03838	3267,58
11	0,5936	0,0936	0,0400	0,00780	0,00053	14,71987	3266,60
12	0,6436	0,1436	0,0500	0,01104	0,00053	20,82862	3265,43
13	0,7136	0,2136	0,0700	0,01481	0,00053	27,94271	3264,06
14	0,8036	0,3036	0,0900	0,01869	0,00053	35,26825	3262,98
15	0,9036	0,4036	0,1000	0,02209	0,00053	41,69625	3261,81
16	1,0036	0,5036	0,1000	0,02482	0,00053	46,84326	3260,63

K	4,62 M^{-1}
Error	0,2902746 M^{-1}

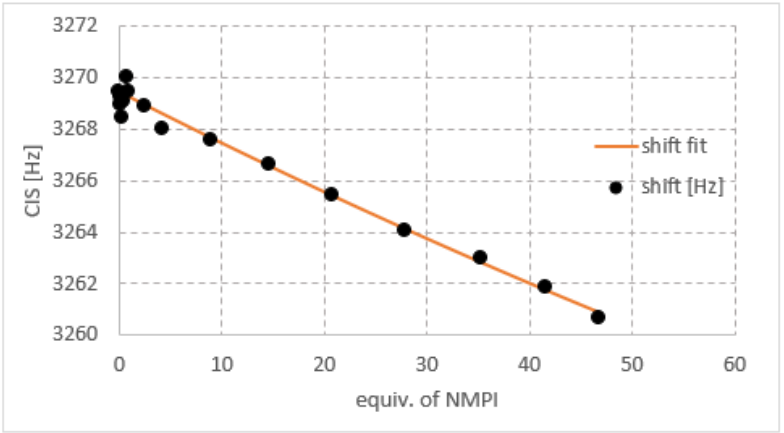

Figure S39: ^{1}H NMR titration of compound **7c** with NMPI ($C_2D_2Cl_4$, 400 MHz).

Calixarene **7d** was dissolved in a specified amount of $C_2D_2Cl_4$. 0.5 ml of calixarene solution was put in an NMR tube. To the calixarene solution (0.6 ml), a specific amount of *N*-methylisoquinolinium iodide (NMII) was added. The aliquots of NMII were gradually added to the NMR tube to achieve different calixarene/guest ratios (1:0.000-50.694), ensuring constant host concentration during the experiment. The complexation constant was determined by analyzing CIS of host protons using nonlinear curve-fitting procedure (program BindFit).

M(NMII)	271,10147 g/mol	M(calix)	739,953 g/mol	
m(NMII)	0,00818 g	m(calix)	0,00221 g	
c(NMII)	0,05029 mol/l	c(calix)	0,00050 mol/l	
V(C2D2Cl4_NMII)	0,6 ml	V(C2D2Cl4_cali	6 ml	

	V (total) [m	V(addition, total) [n	V(addition) [ml]	c(NMII) [mol/l]	c(calix) [mol/l]	c(calix)/c(NM	shift [Hz]	shift 2 [Hz	shift 3 [Hz
1	0,5000	0,0000	0,0000	0,00000	0,00050	0,00000	3269,14	3227,47	3184,14
2	0,5006	0,0006	0,0006	0,00006	0,00050	0,12109	3269,14	3227,57	3184,34
3	0,5012	0,0012	0,0006	0,00012	0,00050	0,24188	3269,63	3227,87	3184,53
4	0,5020	0,0020	0,0008	0,00020	0,00050	0,40249	3269,05	3227,87	3184,63
5	0,5028	0,0028	0,0008	0,00028	0,00050	0,56260	3269,44	3227,77	3184,44
6	0,5042	0,0042	0,0014	0,00042	0,00050	0,84155	3269,34	3228,06	3184,44
7	0,5056	0,0056	0,0014	0,00056	0,00050	1,11896	3269,34	3227,67	3184,24
8	0,5136	0,0136	0,0080	0,00133	0,00050	2,67514	3269,34	3227,57	3184,44
9	0,5236	0,0236	0,0100	0,00227	0,00050	4,55350	3269,14	3227,18	3183,65
10	0,5536	0,0536	0,0300	0,00487	0,00050	9,78142	3268,46	3226,50	3182,68
11	0,5936	0,0936	0,0400	0,00793	0,00050	15,92998	3267,58	3225,81	3182,09
12	0,6436	0,1436	0,0500	0,01122	0,00050	22,54092	3266,89	3225,13	3181,01
13	0,7136	0,2136	0,0700	0,01505	0,00050	30,23985	3266,5	3224,64	3180,33
14	0,8036	0,3036	0,0900	0,01900	0,00050	38,16762	3265,43	3223,86	3179,45
15	0,9036	0,4036	0,1000	0,02246	0,00050	45,12407	3264,94	3223,27	3178,67
16	1,0036	0,5036	0,1000	0,02523	0,00050	50,69421	3264,35	3222,58	3177,88

K	0,17 M^{-1}
Error	0,00635035 M^{-1}

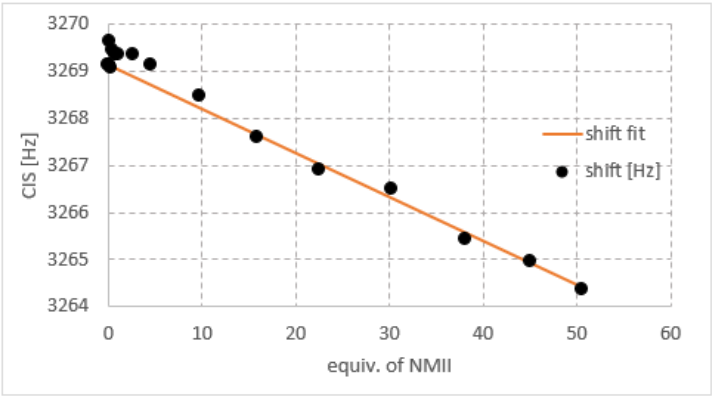

Figure S40: ^{1}H NMR titration of compound **7d** with NMII ($C_2D_2Cl_4$, 400 MHz).

Calixarene **7d** was dissolved in a specified amount of $C_2D_2Cl_4$. 0.5 ml of calixarene solution was put in an NMR tube. To the calixarene solution (0.6 ml), a specific amount of *N*-methylpyridinium iodide (NMPI) was added. The aliquots of NMPI were gradually added to the NMR tube to achieve different calixarene/guest ratios (1:0.000-49.634), ensuring constant host concentration during the experiment. The complexation constant was determined by analyzing CIS of host protons using nonlinear curve-fitting procedure (program BindFit).

M(NMPI)	221,04147 g/mol	M(calix)	739,953 g/mol
m(NMPI)	0,00653 g	m(calix)	0,00221 g
c(NMPI)	0,04924 mol/l	c(calix)	0,00050 mol/l
V(C2D2Cl4_NMPI)	0,6 ml	V(C2D2Cl4_cali	6 ml

	V (total) [m	V(addition, total) [n	V(addition) [ml]	c(NMPI) [mol/l]	c(calix) [mol/l]	c(calix)/c(NM	shift [Hz]	shift 2 [Hz	shift 3 [Hz
1	0,5000	0,0000	0,0000	0,00000	0,00050	0,00000	3276,87	3268,95	3184,24
2	0,5006	0,0006	0,0006	0,00006	0,00050	0,11855	3276,97	3269,24	3184,24
3	0,5012	0,0012	0,0006	0,00012	0,00050	0,23682	3277,26	3269,24	3184,34
4	0,5020	0,0020	0,0008	0,00020	0,00050	0,39407	3277,16	3269,44	3184,44
5	0,5028	0,0028	0,0008	0,00027	0,00050	0,55083	3276,67	3269,63	3184,34
6	0,5042	0,0042	0,0014	0,00041	0,00050	0,82394	3276,77	3269,05	3183,95
7	0,5056	0,0056	0,0014	0,00055	0,00050	1,09555	3277,07	3269,34	3184,14
8	0,5136	0,0136	0,0080	0,00130	0,00050	2,61918	3278,26	3268,75	3183,65
9	0,5236	0,0236	0,0100	0,00222	0,00050	4,45824	3279,41	3267,97	3182,87
10	0,5536	0,0536	0,0300	0,00477	0,00050	9,57679	3280,00	3266,70	3181,50
11	0,5936	0,0936	0,0400	0,00776	0,00050	15,59672	3280,98	3265,23	3180,23
12	0,6436	0,1436	0,0500	0,01099	0,00050	22,06936	3281,47	3264,06	3178,86
13	0,7136	0,2136	0,0700	0,01474	0,00050	29,60722	3282,64	3262,39	3177,10
14	0,8036	0,3036	0,0900	0,01860	0,00050	37,36914	3283,52	3261,12	3176,03
15	0,9036	0,4036	0,1000	0,02199	0,00050	44,18005	3284,01	3260,24	3174,66
16	1,0036	0,5036	0,1000	0,02471	0,00050	49,63367	3284,50	3258,77	3173,87

K	22,28 M^{-1}
Error	0,92069872 M^{-1}

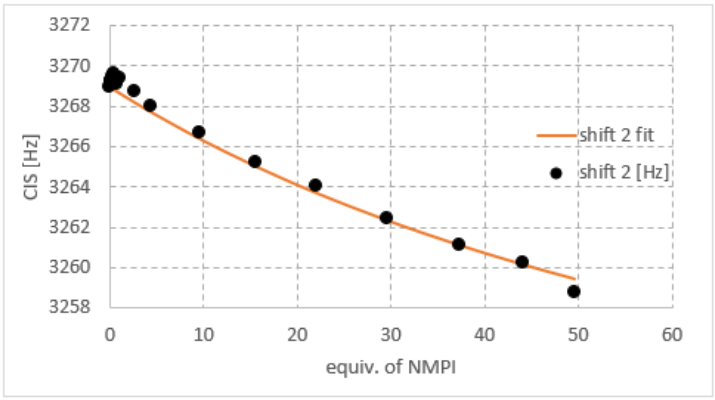

Figure S41: ^{1}H NMR titration of compound **7d** with NMPI ($C_2D_2Cl_4$, 400 MHz).

Calixarene **7d** was dissolved in a specified amount of $C_2D_2Cl_4$. 0.5 ml of calixarene solution was put in an NMR tube. To the calixarene solution (0.6 ml), a specific amount of *N*-methylquinolinium iodide (NMQI) was added. The aliquots of NMQI were gradually added to the NMR tube to achieve different calixarene/guest ratios (1:0.000-50.446), ensuring constant host concentration during the experiment. The complexation constant was determined by analyzing CIS of host protons using nonlinear curve-fitting procedure (program BindFit).

M(NMQI)	271,10147 g/mol		M(calix)	739,953 g/mol
m(NMQI)	0,00814 g		m(calix)	0,00221 g
c(NMQI)	0,05004 mol/l		c(calix)	0,00050 mol/l
V(C2D2Cl4_NMQI)	0,6 ml		V(C2D2Cl4_cali	6 ml

	V (total) [m	V(addition, total) [n	V(addition) [ml]	c(NMQI) [mol/l]	c(calix) [mol/l]	c(calix)/c(NM	shift [Hz]
1	0,5000	0,0000	0,0000	0,00000	0,00050	0,00000	3184,24
2	0,5006	0,0006	0,0006	0,00006	0,00050	0,12049	3184,24
3	0,5012	0,0012	0,0006	0,00012	0,00050	0,24070	3184,44
4	0,5020	0,0020	0,0008	0,00020	0,00050	0,40053	3184,44
5	0,5028	0,0028	0,0008	0,00028	0,00050	0,55984	3184,34
6	0,5042	0,0042	0,0014	0,00042	0,00050	0,83743	3183,75
7	0,5056	0,0056	0,0014	0,00055	0,00050	1,11349	3183,95
8	0,5136	0,0136	0,0080	0,00133	0,00050	2,66206	3184,14
9	0,5236	0,0236	0,0100	0,00226	0,00050	4,53124	3183,56
10	0,5536	0,0536	0,0300	0,00485	0,00050	9,73359	3182,19
11	0,5936	0,0936	0,0400	0,00789	0,00050	15,85208	3181,21
12	0,6436	0,1436	0,0500	0,01117	0,00050	22,43070	3180,23
13	0,7136	0,2136	0,0700	0,01498	0,00050	30,09198	3179,06
14	0,8036	0,3036	0,0900	0,01891	0,00050	37,98099	3177,88
15	0,9036	0,4036	0,1000	0,02235	0,00050	44,90341	3177,10
16	1,0036	0,5036	0,1000	0,02511	0,00050	50,44632	3176,42

K	12,89 M^{-1}
Error	0,50401189 M^{-1}

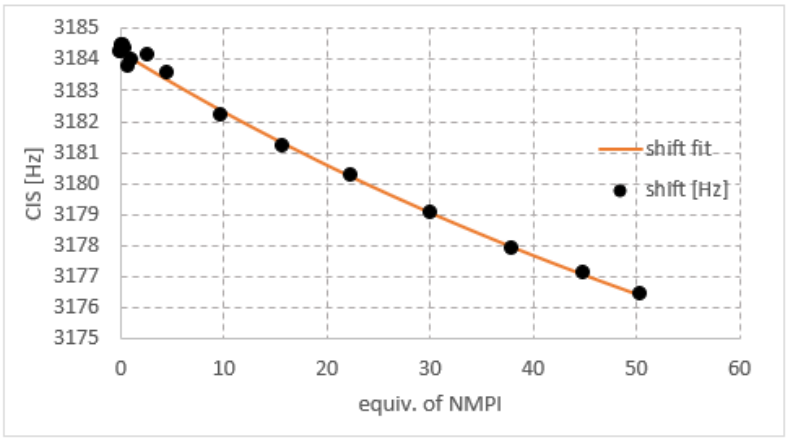

Figure S42: ^{1}H NMR titration of compound **7d** with NMQI ($C_2D_2Cl_4$, 400 MHz).

5. Theoretical calculations

DFT scan (B3LYP/6-31G+)[1] of the rotation around the N-C(=O) bond for **7a** and **8a**/**8b** revealed three possible ways of how this rotation can happen: a) The carbonyl group bends out of the cavity, resulting in the nitrogen atom adopting classical sp^3 hybridization. In this conformation, the rotation around the N-C(=O) bond is not significantly prevented and, thus, the carbonyl part of the molecule can rotate. b) Either the carbonyl oxygen or the methyl of the carbonyl group moves inside the cavity and escapes it on the opposite side. c) A combination of the other two consists in bending the carbonyl group out of the cavity, half-rotation, bending back, which results in the presence of the carbonyl oxygen or the methyl in the cavity, and the finalization of the rotation (or *vice versa*). However, although all the three ways are potentially possible, the calculations did not reveal a simple way for the rotation by either a) or b) mechanism: in the calculated maxima, the geometry always transformed from the a)-like structure to the b)-like structure (or *vice versa*). Thus, the c) mechanism is the most probable one.

In the case of **7a**, the rotation is less energetically demanding when the carbonyl oxygen rotates above the cavity (i.e. the methyl rotates in the close proximity to the bridging methylene): the energy difference between these rotations is ca. 20 kJ/mol. In the more favoured case, the energetic maximum of the rotation is represented by the transition state for the interconversion between the a)-like and the b)-like structure (calculated relative energy 67.6 kJ/mol, which is in a good agreement with the experimental 62 kJ/mol, Figure S43).

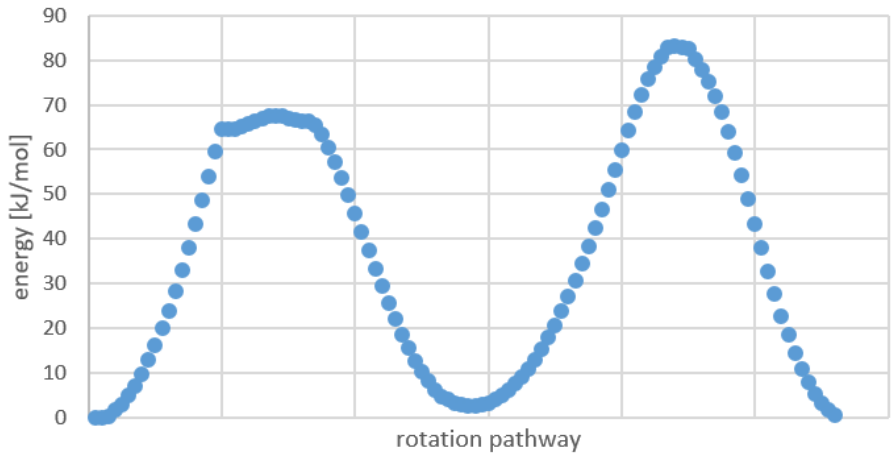

Figure S43: Rotation pathway for compound **7a**

Conversely, in the case of **8a**/**8b**, the energy difference for the oxygen-above-cavity and methyl-above-cavity rotation is small (ca. 4 kJ/mol in favour to methyl-above-cavity pathway). This may be caused by the destabilization of the structure when the bromine and the oxygen atom get to a close proximity. The calculated activation energy for the methyl-above-cavity rotation is ca. 86 kJ/mol (Figure S44). As

expected from the NMR studies, the calculated activation energy for this rotation is much higher to that for the rotation of **7a**. This value also shows, that **8a**/**8b** can be described as atropisomers (it exceeds the value 83.6 kJ/mol generally considered as the border of atropisomerism at room temperature[2]).

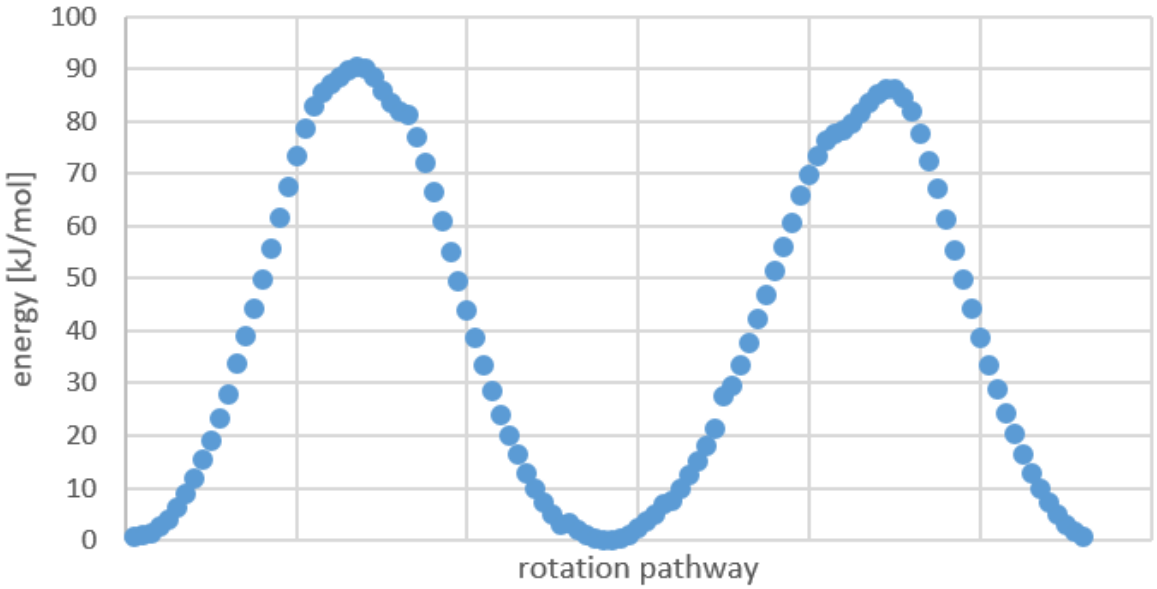

Figure S44: Rotation pathway for compounds **8a**/**8b** (B3LYP/6-31G+)

Table S1: Energies calculated by scan of dihedral angle values of **7a** (B3LYP/6-31G+, clockwise rotation calculated)

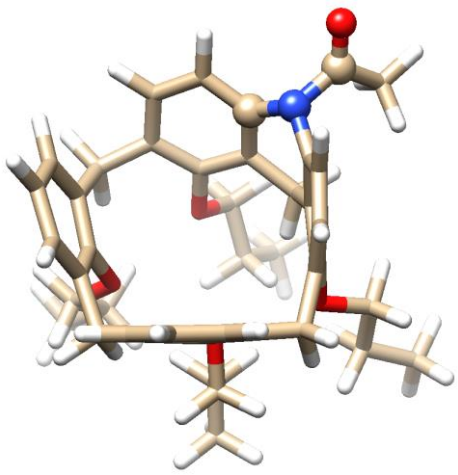

dihedral angle	energy [a.u.]	energy [kJ/mol]	relative energy [kJ/mol]
0.18	-2060.358896	-5408442	0.0735
4.18	-2060.358924	-5408442	0
8.18	-2060.35876	-5408442	0.4305
12.18	-2060.358253	-5408440	1.761375

16.18	-2060.357737	-5408439	3.115875
20.18	-2060.357053	-5408437	4.911375
24.18	-2060.356207	-5408435	7.132125
28.18	-2060.355197	-5408432	9.783375
32.18	-2060.354026	-5408429	12.85725
36.18	-2060.352712	-5408426	16.3065
40.18	-2060.351261	-5408422	20.11538
44.18	-2060.349807	-5408418	23.93212
48.18	-2060.348114	-5408414	28.37625
52.18	-2060.346318	-5408409	33.09075
56.18	-2060.344429	-5408404	38.04937
60.18	-2060.342459	-5408399	43.22063
64.18	-2060.340427	-5408394	48.55462
68.18	-2060.338355	-5408388	53.99363
72.18	-2060.336287	-5408383	59.42212
76.18	-2060.334323	-5408378	64.57762
80.18	-2060.332555	-5408373	69.21862
84.18	-2060.330978	-5408369	73.35825
88.18	-2060.335869	-5408382	60.51938
92.18	-2060.337101	-5408385	57.28537
96.18	-2060.33846	-5408388	53.718
100.18	-2060.339912	-5408392	49.9065
104.18	-2060.341554	-5408397	45.59625
108.18	-2060.343109	-5408401	41.51438
112.18	-2060.344669	-5408405	37.41937
116.18	-2060.346204	-5408409	33.39
120.18	-2060.347698	-5408413	29.46825
124.18	-2060.349141	-5408416	25.68037
128.18	-2060.350512	-5408420	22.0815
132.18	-2060.351793	-5408423	18.71888
136.18	-2060.352976	-5408427	15.6135
140.18	-2060.354051	-5408429	12.79163
144.18	-2060.355004	-5408432	10.29
148.18	-2060.355825	-5408434	8.134875
152.18	-2060.356511	-5408436	6.334125
156.18	-2060.357069	-5408437	4.869375
160.18	-2060.357332	-5408438	4.179
164.18	-2060.357638	-5408439	3.37575
168.18	-2060.357817	-5408439	2.905875
172.18	-2060.357874	-5408439	2.75625
176.18	-2060.357818	-5408439	2.90325
180.18	-2060.357655	-5408439	3.331125
184.18	-2060.35739	-5408438	4.02675
188.18	-2060.35703	-5408437	4.97175
192.18	-2060.356579	-5408436	6.155625
196.18	-2060.356043	-5408435	7.562625

200.18	-2060.355429	-5408433	9.174375
204.18	-2060.354729	-5408431	11.01187
208.18	-2060.353938	-5408429	13.08825
212.18	-2060.353055	-5408427	15.40612
216.18	-2060.352083	-5408424	17.95762
220.18	-2060.351021	-5408421	20.74537
224.18	-2060.349861	-5408418	23.79037
228.18	-2060.348602	-5408415	27.09525
232.18	-2060.347242	-5408412	30.66525
236.18	-2060.34583	-5408408	34.37175
240.18	-2060.344332	-5408404	38.304
244.18	-2060.342763	-5408400	42.42262
248.18	-2060.341142	-5408395	46.67775
252.18	-2060.339491	-5408391	51.01162
256.18	-2060.337821	-5408387	55.39537
260.18	-2060.336144	-5408382	59.7975
264.18	-2060.334485	-5408378	64.15238
268.18	-2060.332883	-5408374	68.35763
272.18	-2060.331375	-5408370	72.31612
276.18	-2060.330002	-5408366	75.92025
280.18	-2060.328812	-5408363	79.044
284.18	-2060.327868	-5408361	81.522
288.18	-2060.32725	-5408359	83.14425
292.18	-2060.327072	-5408359	83.6115
296.18	-2060.336366	-5408383	59.21475
300.18	-2060.338301	-5408388	54.13538
304.18	-2060.340327	-5408393	48.81713
308.18	-2060.342384	-5408399	43.4175
312.18	-2060.344422	-5408404	38.06775
316.18	-2060.346411	-5408409	32.84663
320.18	-2060.348315	-5408414	27.84862
324.18	-2060.35024	-5408419	22.7955
328.18	-2060.351895	-5408424	18.45113
332.18	-2060.3534	-5408428	14.5005
336.18	-2060.354743	-5408431	10.97512
340.18	-2060.355908	-5408434	7.917
344.18	-2060.356884	-5408437	5.355
348.18	-2060.357669	-5408439	3.294375
352.18	-2060.358267	-5408440	1.724625
356.18	-2060.358677	-5408442	0.648375

Table S2: Energies calculated by scan of dihedral angle values of **7a** (B3LYP/6-31G+, anticlockwise rotation calculated)

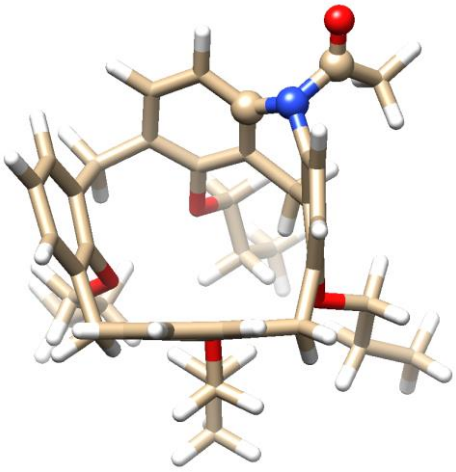

dihedral angle	energy [a.u.]	energy [kJ/mol]	relative energy [kJ/mol]
0.18	-2060.36	-5408442	0.0735
4.18	-2060.36	-5408442	0
8.18	-2060.36	-5408442	0.4305
12.18	-2060.36	-5408440	1.761375
16.18	-2060.36	-5408439	3.115875
20.18	-2060.36	-5408437	4.911375
24.18	-2060.36	-5408435	7.132125
28.18	-2060.36	-5408432	9.783375
32.18	-2060.35	-5408429	12.85725
36.18	-2060.35	-5408426	16.3065
40.18	-2060.35	-5408422	20.11538
44.18	-2060.35	-5408418	23.93212
48.18	-2060.35	-5408414	28.37625
52.18	-2060.35	-5408409	33.09075
56.18	-2060.34	-5408404	38.04937
60.18	-2060.34	-5408399	43.22063
64.18	-2060.34	-5408394	48.55462
68.18	-2060.34	-5408388	53.99363
72.18	-2060.34	-5408383	59.42212
76.18	-2060.33	-5408376	66.255
80.18	-2060.33	-5408377	65.352
84.18	-2060.33	-5408379	63.25988
88.18	-2060.34	-5408382	60.51938
92.18	-2060.34	-5408385	57.28537
96.18	-2060.34	-5408388	53.718
100.18	-2060.34	-5408392	49.9065
104.18	-2060.34	-5408397	45.59625
108.18	-2060.34	-5408401	41.51438
112.18	-2060.34	-5408405	37.41937
116.18	-2060.35	-5408409	33.39

120.18	-2060.35	-5408413	29.46825
124.18	-2060.35	-5408416	25.68037
128.18	-2060.35	-5408420	22.0815
132.18	-2060.35	-5408423	18.71888
136.18	-2060.35	-5408427	15.6135
140.18	-2060.35	-5408429	12.79163
144.18	-2060.36	-5408432	10.29
148.18	-2060.36	-5408434	8.134875
152.18	-2060.36	-5408436	6.334125
156.18	-2060.36	-5408437	4.869375
160.18	-2060.36	-5408438	4.179
164.18	-2060.36	-5408439	3.37575
168.18	-2060.36	-5408439	2.905875
172.18	-2060.36	-5408439	2.75625
176.18	-2060.36	-5408439	2.90325
180.18	-2060.36	-5408439	3.331125
184.18	-2060.36	-5408438	4.02675
188.18	-2060.36	-5408437	4.97175
192.18	-2060.36	-5408436	6.155625
196.18	-2060.36	-5408435	7.562625
200.18	-2060.36	-5408433	9.174375
204.18	-2060.35	-5408431	11.01187
208.18	-2060.35	-5408429	13.08825
212.18	-2060.35	-5408427	15.40612
216.18	-2060.35	-5408424	17.95762
220.18	-2060.35	-5408421	20.74537
224.18	-2060.35	-5408418	23.79037
228.18	-2060.35	-5408415	27.09525
232.18	-2060.35	-5408412	30.66525
236.18	-2060.35	-5408408	34.37175
240.18	-2060.34	-5408404	38.304
244.18	-2060.34	-5408400	42.42525
248.18	-2060.34	-5408395	46.67775
252.18	-2060.34	-5408391	51.01162
256.18	-2060.33	-5408359	82.6875
260.18	-2060.33	-5408360	82.62188
264.18	-2060.33	-5408360	82.089
268.18	-2060.33	-5408361	81.26212
272.18	-2060.33	-5408362	80.14912
276.18	-2060.33	-5408364	77.8785
280.18	-2060.33	-5408367	75.20363
284.18	-2060.33	-5408370	71.841
288.18	-2060.33	-5408374	68.33138
292.18	-2060.33	-5408378	63.98437
296.18	-2060.34	-5408383	59.21475
300.18	-2060.34	-5408388	54.13538

304.18	-2060.34	-5408393	48.81713
308.18	-2060.34	-5408399	43.4175
312.18	-2060.34	-5408404	38.06775
316.18	-2060.35	-5408409	32.84663
320.18	-2060.35	-5408414	27.84862
324.18	-2060.35	-5408419	22.7955
328.18	-2060.35	-5408424	18.45113
332.18	-2060.35	-5408428	14.5005
336.18	-2060.35	-5408431	10.97512
340.18	-2060.36	-5408434	7.917
344.18	-2060.36	-5408437	5.355
348.18	-2060.36	-5408439	3.294375
352.18	-2060.36	-5408440	1.724625
356.18	-2060.36	-5408442	0.648375

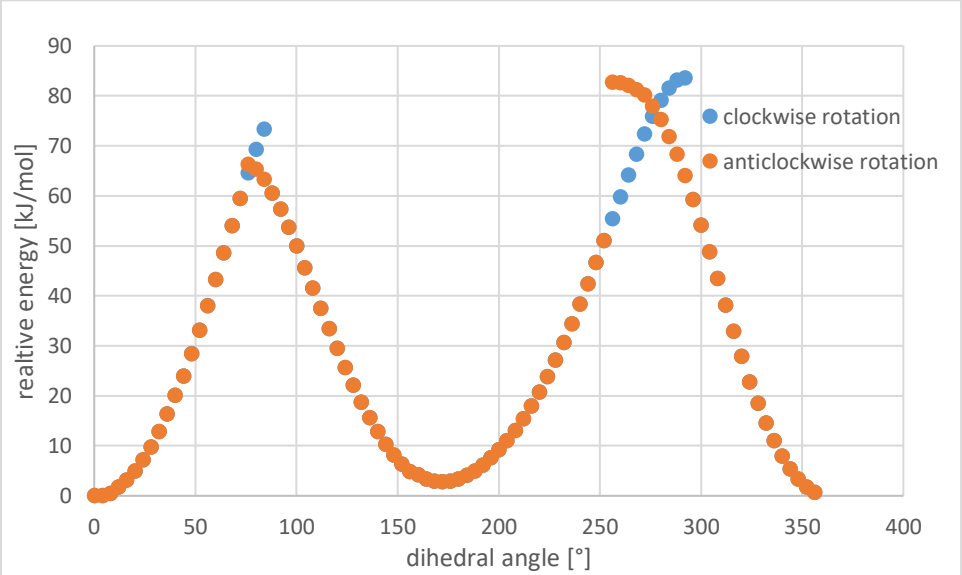

Figure S45: Comparison of clockwise and anticlockwise rotation calculation (compound **7a**)

Table S3: Energies calculated by scan of dihedral angle values of **8a**/**8b** (B3LYP/6-31G+, anticlockwise rotation calculated)

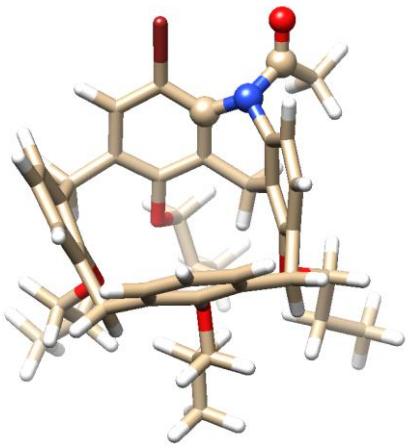

dihedral angle	energy [a.u.]	energy [kJ/mol]	relative energy [kJ/mol]
0.8111	-4631.366896	-12157338.1	0.847875
4.8111	-4631.366884	-12157338.07	0.879375
8.8111	-4631.366675	-12157337.52	1.428
12.8111	-4631.366264	-12157336.44	2.506875
16.8111	-4631.365664	-12157334.87	4.081875
20.8111	-4631.364868	-12157332.78	6.171375
24.81082	-4631.36388	-12157330.19	8.764875
28.81082	-4631.362723	-12157327.15	11.802
32.81082	-4631.361402	-12157323.68	15.26962
36.81082	-4631.359926	-12157319.81	19.14412
40.81017	-4631.35831	-12157315.56	23.38613
44.81017	-4631.356563	-12157310.98	27.972
48.81017	-4631.354338	-12157305.14	33.81262
52.81017	-4631.352378	-12157299.99	38.95762
56.81017	-4631.350327	-12157294.61	44.3415
60.81017	-4631.348194	-12157289.01	49.94062
64.81017	-4631.345991	-12157283.23	55.7235
68.81017	-4631.343748	-12157277.34	61.61137
72.81017	-4631.341503	-12157271.45	67.5045
76.81017	-4631.339302	-12157265.67	73.28212
80.81017	-4631.337273	-12157260.34	78.60825
84.81017	-4631.335644	-12157256.07	82.88438
88.81017	-4631.334232	-12157252.36	86.59087
92.81017	-4631.333097	-12157249.38	89.57025
96.81052	-4631.341666	-12157271.87	67.07662
100.8105	-4631.343825	-12157277.54	61.40925
104.8104	-4631.346037	-12157283.35	55.60275
108.8104	-4631.348244	-12157289.14	49.80937
112.8108	-4631.35038	-12157294.75	44.20237

116.8106	-4631.352352	-12157299.92	39.02587
120.8106	-4631.354312	-12157305.07	33.88087
124.8106	-4631.356152	-12157309.9	29.05087
128.8106	-4631.35786	-12157314.38	24.56737
132.8106	-4631.359427	-12157318.5	20.454
136.8106	-4631.360847	-12157322.22	16.7265
140.8106	-4631.36212	-12157325.57	13.38487
144.8106	-4631.363254	-12157328.54	10.40813
148.8106	-4631.364254	-12157331.17	7.783125
152.8106	-4631.365123	-12157333.45	5.502
156.8106	-4631.365858	-12157335.38	3.572625
160.8106	-4631.366034	-12157335.84	3.110625
164.8106	-4631.36651	-12157337.09	1.861125
168.8106	-4631.366868	-12157338.03	0.921375
172.8106	-4631.367106	-12157338.65	0.296625
176.8106	-4631.367219	-12157338.95	0
180.8106	-4631.367203	-12157338.91	0.042
184.8106	-4631.367058	-12157338.53	0.422625
188.8106	-4631.366787	-12157337.82	1.134
192.8106	-4631.366396	-12157336.79	2.160375
196.8106	-4631.365895	-12157335.47	3.4755
200.8106	-4631.365298	-12157333.91	5.042625
204.8106	-4631.364617	-12157332.12	6.83025
208.8106	-4631.364296	-12157331.28	7.672875
212.811	-4631.363414	-12157328.96	9.988125
216.811	-4631.362479	-12157326.51	12.4425
220.811	-4631.361434	-12157323.76	15.18562
224.811	-4631.360287	-12157320.75	18.1965
228.8108	-4631.359044	-12157317.49	21.45937
232.8108	-4631.356749	-12157311.47	27.48375
236.8108	-4631.356027	-12157309.57	29.379
240.8108	-4631.354488	-12157305.53	33.41887
244.8108	-4631.352863	-12157301.27	37.6845
248.8108	-4631.351168	-12157296.82	42.13387
252.8108	-4631.349416	-12157292.22	46.73287
256.8108	-4631.347635	-12157287.54	51.408
260.8108	-4631.345853	-12157282.86	56.08575
264.8108	-4631.344104	-12157278.27	60.67687
268.8108	-4631.342178	-12157273.22	65.73263
272.8108	-4631.340617	-12157269.12	69.83025
276.8108	-4631.339239	-12157265.5	73.4475
280.8108	-4631.338134	-12157262.6	76.34812
284.8108	-4631.33742	-12157260.73	78.22237
288.8108	-4631.337437	-12157260.77	78.17775
292.8108	-4631.343667	-12157277.13	61.824
296.8108	-4631.345886	-12157282.95	55.99912

300.8108	-4631.34809	-12157288.74	50.21362
304.8108	-4631.350242	-12157294.39	44.56462
308.8108	-4631.352302	-12157299.79	39.15712
312.8108	-4631.354242	-12157304.89	34.06462
316.8111	-4631.356059	-12157309.65	29.295
320.8111	-4631.357756	-12157314.11	24.84037
324.8111	-4631.359329	-12157318.24	20.71125
328.8111	-4631.360779	-12157322.04	16.905
332.8111	-4631.362102	-12157325.52	13.43212
336.8111	-4631.363277	-12157328.6	10.34775
340.8111	-4631.364293	-12157331.27	7.68075
344.8111	-4631.365149	-12157333.52	5.43375
348.8111	-4631.365844	-12157335.34	3.609375
352.8111	-4631.366369	-12157336.72	2.23125
356.8111	-4631.366719	-12157337.64	1.3125

Table S4: Energies calculated by scan of dihedral angle values of **8a**/**8b** (B3LYP/6-31G+, anticlockwise rotation calculated)

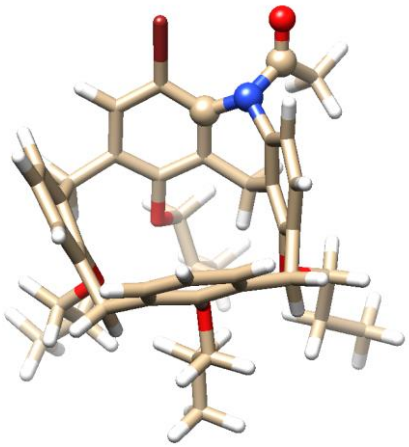

dihedral angle	energy [a.u.]	energy [kJ/mol]	relative energy [kJ/mol]
0.81	-4631.366896	-12157338.1	0.364874998
4.81	-4631.366884	-12157338.07	0.396375
8.81	-4631.366675	-12157337.52	0.944999998
12.81	-4631.366264	-12157336.44	2.023875
16.81	-4631.365664	-12157334.87	3.598874999
20.81	-4631.364868	-12157332.78	5.688375
24.81	-4631.36388	-12157330.19	8.281874999
28.81	-4631.330796	-12157243.34	95.127375
32.81	-4631.331148	-12157244.26	94.203375
36.81	-4631.331377	-12157244.86	93.60225
40.81	-4631.331504	-12157245.2	93.268875
44.81	-4631.331801	-12157245.98	92.48925
48.81	-4631.331774	-12157245.91	92.560125

52.81	-4631.331707	-12157245.73	92.736
56.81	-4631.33165	-12157245.58	92.885625
60.81	-4631.331667	-12157245.63	92.841
64.81	-4631.331851	-12157246.11	92.358
68.81	-4631.33219	-12157247	91.468125
72.81	-4631.332748	-12157248.46	90.003375
76.81	-4631.333574	-12157250.63	87.835125
80.81	-4631.334677	-12157253.53	84.93975
84.81	-4631.336063	-12157257.17	81.3015
88.81	-4631.337723	-12157261.52	76.944
92.81	-4631.339614	-12157266.49	71.980125
96.81	-4631.341667	-12157271.88	66.591
100.81	-4631.343825	-12157277.54	60.92625
104.81	-4631.346038	-12157283.35	55.117125
108.81	-4631.348135	-12157288.85	49.6125
112.81	-4631.350284	-12157294.5	43.971375
116.81	-4631.352353	-12157299.93	38.54025
120.81	-4631.354313	-12157305.07	33.39525
124.81	-4631.356152	-12157309.9	28.567875
128.81	-4631.35786	-12157314.38	24.084375
132.81	-4631.359428	-12157318.5	19.968375
136.81	-4631.360847	-12157322.22	16.2435
140.81	-4631.36212	-12157325.57	12.901875
144.81	-4631.363254	-12157328.54	9.925125001
148.81	-4631.364255	-12157331.17	7.297499999
152.81	-4631.365123	-12157333.45	5.019000001
156.81	-4631.365858	-12157335.38	3.089624999
160.81	-4631.365742	-12157335.07	3.394125
164.81	-4631.36625	-12157336.41	2.060625
168.81	-4631.366643	-12157337.44	1.028999999
172.81	-4631.366902	-12157338.12	0.349125
176.81	-4631.367035	-12157338.47	0
180.81	-4631.316296	-12157205.28	133.189875
184.81	-4631.31825	-12157210.41	128.060625
188.81	-4631.320109	-12157215.29	123.18075
192.81	-4631.321823	-12157219.79	118.6815
196.81	-4631.323348	-12157223.79	114.678375
200.81	-4631.324669	-12157227.26	111.21075
204.81	-4631.325778	-12157230.17	108.299625
208.81	-4631.326682	-12157232.54	105.926625
212.81	-4631.327215	-12157233.94	104.5275
216.81	-4631.327722	-12157235.27	103.196625
220.81	-4631.328055	-12157236.14	102.3225
224.81	-4631.328232	-12157236.61	101.857875
228.81	-4631.328582	-12157237.53	100.939125
232.81	-4631.32875	-12157237.97	100.498125

236.81	-4631.328618	-12157237.62	100.844625
240.81	-4631.328072	-12157236.19	102.277875
244.81	-4631.327949	-12157235.87	102.60075
248.81	-4631.327955	-12157235.88	102.585
252.81	-4631.328446	-12157237.17	101.296125
256.81	-4631.329118	-12157238.93	99.532125
260.81	-4631.329988	-12157241.22	97.248375
264.81	-4631.331064	-12157244.04	94.423875
268.81	-4631.332363	-12157247.45	91.014
272.81	-4631.333895	-12157251.47	86.9925
276.81	-4631.335609	-12157255.97	82.49325
280.81	-4631.337471	-12157260.86	77.6055
284.81	-4631.339477	-12157266.13	72.33975
288.81	-4631.341466	-12157271.35	67.118625
292.81	-4631.343667	-12157277.13	61.341
296.81	-4631.345886	-12157282.95	55.516125
300.81	-4631.34809	-12157288.74	49.730625
304.81	-4631.350242	-12157294.39	44.081625
308.81	-4631.352302	-12157299.79	38.674125
312.81	-4631.354242	-12157304.89	33.581625
316.81	-4631.356059	-12157309.65	28.812
320.81	-4631.357756	-12157314.11	24.357375
324.81	-4631.359329	-12157318.24	20.22825
328.81	-4631.360779	-12157322.04	16.422
332.81	-4631.362102	-12157325.52	12.949125
336.81	-4631.363277	-12157328.6	9.86475
340.81	-4631.364293	-12157331.27	7.19775
344.81	-4631.365149	-12157333.52	4.950749999
348.81	-4631.365844	-12157335.34	3.126375001
352.81	-4631.366369	-12157336.72	1.748249998
356.81	-4631.366719	-12157337.64	0.829500001

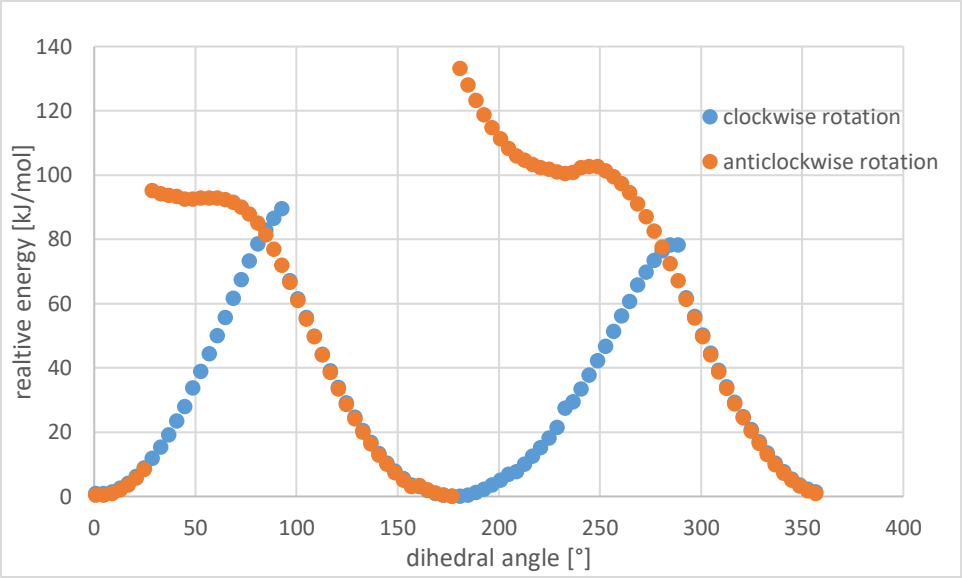

Figure S46: Comparison of clockwise and anticlockwise rotation calculation (compounds **8a**/**8b**)

Table S5: Energies calculated by scan of angle values of **7a** (B3LYP/6-31G+, oxygen in the cavity)

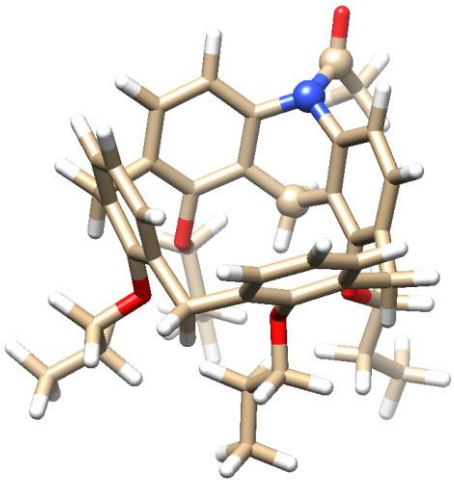

dihedral angle	energy [a.u.]	energy [kJ/mol]	relative energy [kJ/mol]
163.38	-2060.33	-5408376	66.255
159.38	-2060.33	-5408376	66.507
155.38	-2060.33	-5408375	67.02412
151.38	-2060.33	-5408375	67.47038
147.38	-2060.33	-5408375	67.59637
143.38	-2060.33	-5408375	67.431
139.38	-2060.33	-5408375	67.00838
135.38	-2060.33	-5408376	66.3915
131.38	-2060.33	-5408376	65.68538
127.38	-2060.33	-5408377	65.04488
123.38	-2060.33	-5408377	64.68262
119.38	-2060.33	-5408378	64.575

Table S6: Energies calculated by scan of angle values of **7a** (B3LYP/6-31G+, methyl in the cavity)

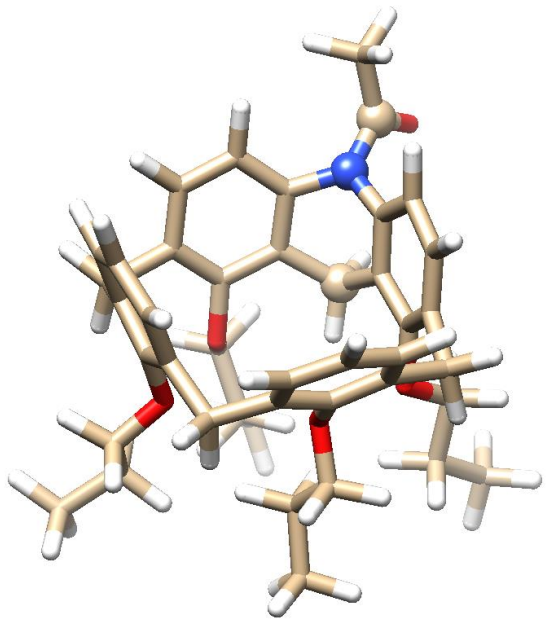

dihedral angle	energy [a.u.]	energy [kJ/mol]	relative energy [kJ/mol]
160.05	-2060.327425	-5408359	82.68488
156.05	-2060.327361	-5408359	82.85287
152.05	-2060.327304	-5408359	83.0025
148.05	-2060.327351	-5408359	82.87912
144.05	-2060.327638	-5408360	82.12575
140.05	-2060.328205	-5408362	80.63738
136.05	-2060.329034	-5408364	78.46125
132.05	-2060.330027	-5408366	75.85462
128.05	-2060.331267	-5408370	72.59962

Table S7: Energies calculated by scan of angle values of **8a**/**8b** (B3LYP/6-31G+, oxygen in the cavity)

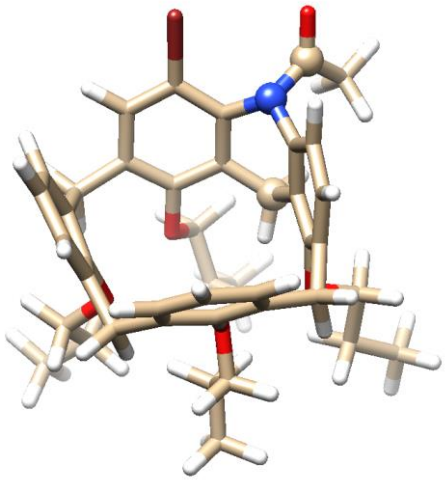

dihedral angle	energy [a.u.]	energy [kJ/mol]	relative energy [kJ/mol]
109.563	-4631.335644	-12157256.07	82.40138
113.563	-4631.335805	-12157256.49	81.97875
117.563	-4631.335211	-12157254.93	83.538
121.563	-4631.334348	-12157252.66	85.80337
125.563	-4631.333361	-12157250.07	88.39425
129.563	-4631.332717	-12157248.38	90.08475
133.563	-4631.332625	-12157248.14	90.32625
137.563	-4631.332861	-12157248.76	89.70675
141.563	-4631.333313	-12157249.95	88.52025
145.563	-4631.333861	-12157251.39	87.08175
149.563	-4631.334429	-12157252.88	85.59075
153.563	-4631.334994	-12157254.36	84.10763
157.563	-4631.335603	-12157255.96	82.509

Table S9: Energies calculated by scan of angle values of **8a**/**8b** (B3LYP/6-31G+, methyl in the cavity)

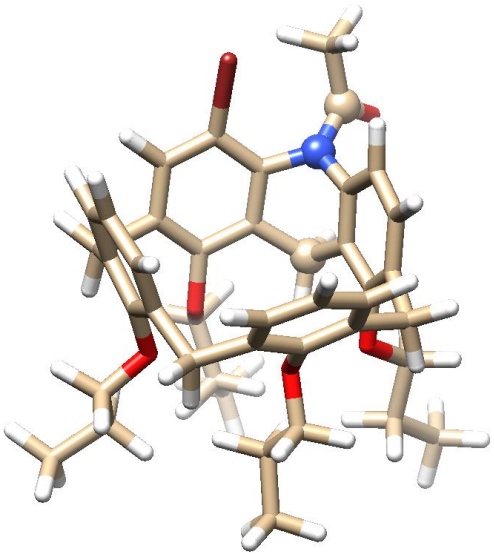

dihedral angle	energy [a.u.]	energy [kJ/mol]	relative energy [kJ/mol]
112.39	-4631.335842	-12157256.59	81.881625
116.39	-4631.334824	-12157253.91	84.553875
120.39	-4631.334221	-12157252.33	86.13675
124.39	-4631.334189	-12157252.25	86.22075
128.39	-4631.334604	-12157253.34	85.131375
132.39	-4631.335227	-12157254.97	83.496
136.39	-4631.33598	-12157256.95	81.519375
140.39	-4631.33668	-12157258.79	79.681875
144.39	-4631.337232	-12157260.23	78.232875
148.39	-4631.337471	-12157260.86	77.6055

(1) Gaussian 16, Revision C.01, M. J. Frisch, G. W. Trucks, H. B. Schlegel, G. E. Scuseria, M. A. Robb, J. R. Cheeseman, G. Scalmani, V. Barone, G. A. Petersson, H. Nakatsuji, X. Li, M. Caricato, A. V. Marenich, J. Bloino, B. G. Janesko, R. Gomperts, B. Mennucci, H. P. Hratchian, J. V. Ortiz, A. F. Izmaylov, J. L. Sonnenberg, D. Williams-Young, F. Ding, F. Lipparini, F. Egidi, J. Goings, B. Peng, A. Petrone, T. Henderson, D. Ranasinghe, V. G. Zakrzewski, J. Gao, N. Rega, G. Zheng, W. Liang, M. Hada, M. Ehara, K. Toyota, R. Fukuda, J. Hasegawa, M. Ishida, T. Nakajima, Y. Honda, O. Kitao, H. Nakai, T. Vreven, K. Throssell, J. A. Montgomery, Jr., J. E. Peralta, F. Ogliaro, M. J. Bearpark, J. J. Heyd, E. N. Brothers, K. N. Kudin, V. N. Staroverov, T. A. Keith, R. Kobayashi, J. Normand, K. Raghavachari, A. P. Rendell, J. C. Burant, S. S. Iyengar, J. Tomasi, M. Cossi, J. M. Millam, M. Klene, C. Adamo, R. Cammi, J. W. Ochterski, R. L. Martin, K. Morokuma, O. Farkas, J. B. Foresman, and D. J. Fox, Gaussian, Inc., Wallingford CT, 2016.

(2) S. R. LaPlante, P. J. Edwards, L. D. Fader, A. Jakalian and O. Hucke, *ChemMedChem,* 2011, ***6***, 505-513.